# Multistage growth and compositional change at the Goat Rocks volcanic complex, a major Pliocene-Pleistocene andesite center in the southern Washington Cascades

Kellie T. Wall Anita L. Grunder Daniel P. Miggins

College of Earth, Ocean, and Atmospheric Sciences, Oregon State University, 104 CEOAS Administration Building, Corvallis, Oregon 97331, USA

#### Matthew A. Coble

Department of Geological Sciences, Stanford University, 367 Panama Street Room 89, Stanford, California 94305, USA

#### ABSTRACT

The deeply eroded Goat Rocks volcanic complex was a major locus of andesitic volcanism in the Cascade arc in southwest Washington during the late Pliocene to Pleistocene. This volcanic complex includes the remnants of multiple andesitic edifices over an area of ~200 km<sup>2</sup>, centered ~35 km north of Mount Adams on the arc axis. New 40Ar/39Ar ages for seven samples and U/Pb zircon ages for nine samples indicate a 2.5–2.9 m.y. eruptive history at Goat Rocks. Four eruptive stages are delineated: Tieton Peak (potentially 3.0-2.6 Ma), Bear Creek Mountain (>1.6-1.3 Ma), Lake Creek (1.1-0.6 Ma), and Old Snowy Mountain (0.4-0.1 Ma), each named for the major vent that was active during that time. Lake Creek volcano was the most voluminous of these edifices and probably rose at least 3400 m above sea level with a volume of ~60 km<sup>3</sup>, comparable to nearby active composite volcanoes. Thirty new bulk composition X-ray fluorescence (XRF) and inductively coupled plasma-mass spectrometry analyses from the volcanic complex are presented, in addition to 54 previously unpublished XRF analyses for samples collected by Don Swanson. The compositional variability is greatest in the early and late stages, ranging from basaltic andesite to rhyolite, whereas the more voluminous middle stages are dominated by andesite to dacite. The middle eruptive stages are interpreted to have been a time of peak thermal energy with a mature subvolcanic plexus. In addition, compositions shift from high-K to medium-K compositions with time, which mimics variation across the arc; early eruptive products are similar in composition to those of Mount Adams, and Old Snowy Mountain stage compositions are more similar to those of Mount St. Helens. The life cycle of Goat Rocks volcanic complex provides new perspective on the longevity and evolution of major arc volcanoes, and on the complex distribution of magma in the Cascade arc at the latitudes of southern Washington and adjacent Oregon.

Wall, K.T., Grunder, A.L., Miggins, D.P., and Coble, M.A., 2018, Multistage growth and compositional change at the Goat Rocks volcanic complex, a major Pliocene–Pleistocene andesite center in the southern Washington Cascades, *in* Poland, M.P., Garcia, M.O., Camp, V.E., and Grunder, A., eds., Field Volcanology: A Tribute to the Distinguished Career of Don Swanson: Geological Society of America Special Paper 538, p. 63–91, https://doi.org/10.1130/2018.2538(04). © 2018 The Geological Society of America. All rights reserved. For permission to copy, contact editing@geosociety.org.

#### INTRODUCTION

A distinctive feature of convergent margins is the magnificent active volcanoes of "orogenic andesite" (Gill, 1981), which inspire art and legends, provide recreation and resources, and threaten life and property. Arc andesite centers, in the form of individual volcanoes or volcanic clusters, are spaced several tens to a few hundred kilometers along subduction zones. This alongarc spacing has been modeled to result from distributed buoyant rise of mantle from the deep mantle wedge (e.g., de Bremond d'Ars et al., 1995; Tamura et al., 2001), a response to lithospheric thickness (e.g., ten Brink, 1991), and/or crustal influences (Savant and de Silva, 2005). The productivity, timing, and composition of arc volcanoes inform the balance of geochemical cycling in subduction zones. Arc volcanoes have typical life spans of a few tens of thousands of years to a few hundred thousand years, whereas clusters of volcanoes have life spans ranging from ~1 m.y. to more than 10 m.y. (Jicha and Singer, 2006; Grunder et al., 2006). Many basic facts remain to be assembled about the distribution, longevity, and geochemical evolution of arc volcanoes before arc-scale models of subduction zone magmatism can be tested.

The focus in this paper is on the Cascade arc, which, despite its modest length of 1250 km, features great variety in setting and composition among its 22 broadly andesitic Quaternary arc volcanoes (see compilation by Hildreth, 2007). In the central segment of the arc (southern Washington to northern Oregon), the arc front is not linear, as it is to the north and south. Instead, the volcanoes Mount St. Helens and Mount Rainier lie trenchward of the arc axis defined by Mount Hood and Mount Adams; farther east lies the alkalic Simcoe volcanic field (Fig. 1). Compositions are generally more alkalic with distance from the trench (Leeman et al., 1990, 2005). In addition, the volcanoes in this arc segment exhibit variable eruptive histories and behavior. Mount Hood, for example, has a history dating back to ca. 3.1 Ma and has infrequently erupted silicic andesite to mafic dacite (i.e., quite monotonous) lavas over the last several thousand years (Wise, 1969; Sherrod and Scott, 1995; Scott and Gardner, 2017). In contrast, Mount St. Helens is a relative newcomer to the arc, having initiated ~300,000 yr ago, and it has had frequent explosive eruptions ranging in composition from basalt to dacite (Mullineaux and Crandell, 1981; Clynne et al., 2008). To give perspective to the distribution, longevity, and relative timing of volcanoes in this segment of the arc, as well as the spatial and temporal variation in their compositions, we turned our attention to the age and compositional record of the Goat Rocks volcanic complex ("Goat Rocks," for short), a young but extinct cluster of andesitic volcanoes located approximately within the Goat Rocks Wilderness of Washington State (Fig. 1).

New age determinations for 13 samples from Goat Rocks, including <sup>40</sup>Ar/<sup>39</sup>Ar ages for seven samples and U/Pb ages for nine samples, provide a geochronological framework that augments mapping and age relations established by other authors (Swanson and Clayton, 1983; Clayton, 1983; Swanson, 1996a, 1996b; Hammond, 2017; Gusey et al., this volume). Goat Rocks

was active as recently as ~100,000 yr ago and was a major andesitic locus over a period of at least 2.5 m.y., and possibly as long as 2.9 m.y. Goat Rocks reached its maximum volcanic output in its third of four eruptive stages, overlapping in time with the construction of ancestral Mount Rainier and Mount Hood. Activity at Goat Rocks waned as Mount Adams and Mount St. Helens emerged.

Changes through time in compositions erupted at Goat Rocks are illustrated by 30 new and 54 previously unpublished bulk rock compositional analyses presented in this paper. Early volcanism was compositionally similar to the medium-K to high-K suite of Mount Adams, while late-stage eruptions were least

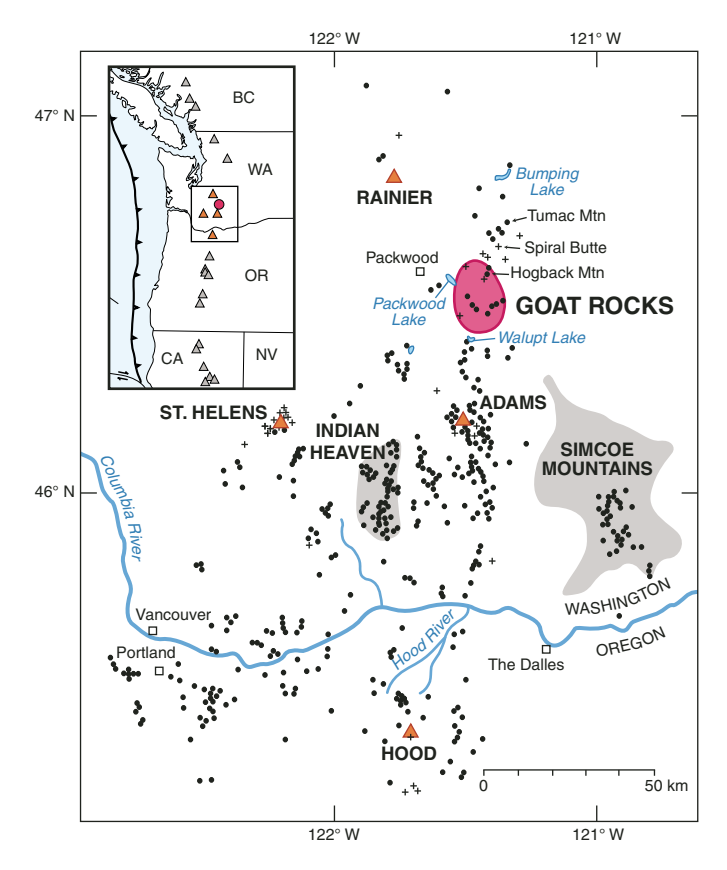


Figure 1. Map of the Mount Rainier to Mount Hood region of the Cascade arc. Inset shows location in the Cascade arc, which spans from British Columbia to California. Orange triangles are major Quaternary composite volcanoes Mount Rainier, Mount Adams, Mount St. Helens, and Mount Hood. The areal extent (andesitic footprint) of the Goat Rocks volcanic complex (including all Pliocene to Pleistocene andesite-dacite vents) is shown by the pink field (pink circle on inset map). Gray triangles on inset map are other major Quaternary edifices after Hildreth (2007). Gray fields show extent of distributed Indian Heaven and Simcoe Mountains mafic fields. Black dots are locations of Quaternary basaltic to andesitic vents; crosses are dacitic to rhyolitic vents. The Goat Rocks field includes two extinct Pliocene vents at Tieton Peak and Devils Washbasin. Figure is modified from Hildreth (2007) with updated locations of vents in Goat Rocks volcanic complex. BC—British Columbia, WA—Washington, OR—Oregon, CA— California, NV—Nevada.

potassic and most adakite-like, similar to compositions of Mount St. Helens. The compositional variation at Goat Rocks through time thus mimics the compositional variation observed across the arc in this segment of the Cascades.

#### **Geologic Setting**

Goat Rocks volcanic complex is part of the Cascade volcanic arc, which extends 1250 km from British Columbia to California and includes >2300 Quaternary volcanoes related to subduction of the Explorer, Juan de Fuca, and Gorda plates beneath the North American plate (Fig. 1; Hildreth, 2007). Goat Rocks is the northernmost major volcanic center on the main arc axis that extends from Crater Lake in southern Oregon, through the Oregon Cascades and Mount Adams in southern Washington, and passes through Goat Rocks toward Bumping Lake (Fig. 1). Neighboring major arc volcanoes Mount Rainier and Mount St. Helens are offset to the west, and the Simcoe mafic volcanic field lies to the east (Fig. 1).

The Rainier-to-Hood segment of the Cascade arc is geomorphologically distinct; abundant mafic volcanic vents and major andesitic centers span ~160 km across the arc (Fig. 1; Guffanti and Weaver, 1988; Hildreth, 2007). The region lies at a major structural transition between extension to the south and compression to the north. To the south, clockwise rotation of the Oregon Coast Range (Wells et al., 1998; Wells and McCaffrey, 2013) has led to eastward migration of the Oregon arc through time, and east-west extension affects the present arc (Hughes and Taylor, 1986; Conrey et al., 2002, 2004). To the north, northeasterly compression prevails, and the position of the arc axis has been relatively fixed, with minor westward migration (see vent loci in Hildreth, 2007).

The crust beneath the southern Washington Cascades is 40-45 km thick (Shen et al., 2013). Underlying the Cascade arc volcanic products, there is a patchwork of Paleozoic to Eocene accreted terranes, including Paleozoic to Mesozoic mélange belts (Miller, 1989) and the early Paleogene Siletz terrane, a fossil oceanic plateau that crops out in the Washington and Oregon forearc and may underlie the arc (Trehu et al., 1994; Wells et al., 2014). In addition, the locations of Goat Rocks and neighboring Mount Rainier, Mount Adams, and Mount St. Helens coincide with the Southern Washington Cascades conductor, a complex conductive feature (Stanley et al., 1987; Hill et al., 2009). Recent highresolution magnetotelluric studies (e.g., Bowles-Martinez et al., 2016) have revealed a complex network of midcrustal conductive regions near and between the major volcanic centers. These conductive areas have been interpreted as regions of melting and (or) fluid or sulfide-rich metasedimentary layers (Stanley et al., 1987; Hill et al., 2009; Bowles-Martinez et al., 2016).

Like elsewhere in the Cascade arc, multiple primitive magma types have erupted throughout the Rainier-to-Hood section, including calk-alkaline basalt and low-K tholeiite (Bacon et al., 1997, Conrey et al., 1997), as well as intraplate basalts (Leeman et al., 2005). The latter are a distinctive component

of this segment of the arc (Schmidt et al., 2008). Mullen et al. (2017) used Pb, Hf, Nd, and Sr isotope characteristics to define the High Cascades (Mount Rainier to Lassen Peak) as a single arc segment, albeit with a distinct array for Mount Adams and the Simcoe volcanic field. The major volcanic centers from Mount Rainier to Mount Hood have distinct geochemical compositions, with K<sub>2</sub>O and other incompatible element concentrations being generally lower at a given SiO<sub>2</sub> in the forearc (Mount St. Helens), higher on the arc (Mount Adams), and highest in the back-arc (Simcoe volcanic field; Leeman et al., 1990).

#### **Previous Work**

Our present understanding of Goat Rocks volcanic complex is the culmination of more than a century of geologic research. In 1893, during reconnaissance field work, U.S. Geological Survey (USGS) geologist Israel C. Russell discovered a thick outcrop of columnar andesite on the bank of the Naches River that he inferred to be a lava flow from "somewhere in the elevated region drained by Tiaton [sic] creek" (1893, p. 64). Smith (1903) named the great lava flow the Tieton (pronounced tī-eton) andesite. Later, Ellingson (1968) proposed that its source was a volcanic plug at the peak called Black Thumb, west of Gilbert Peak (Fig. 2). Noting the similarity of the Tieton andesite to other pyroxene andesite lava flows exposed in the Goat Rocks area, Ellingson (1968) envisioned that Black Thumb had been the center of a major composite volcano, the Goat Rocks volcano, which stood >12,000 ft (3650 m) tall prior to its destruction by glacial erosion.

Clayton (1983) investigated the Devils Horns rhyolite, a thick sequence of (probably caldera-filling) rhyolite tuff, lava flows, and breccias that crops out on the east side of Goat Rocks. Two samples from this rhyolite sequence yielded zircon fissiontrack ages of 3.20  $\pm$  0.14 Ma and 3.17  $\pm$  0.16 Ma (Clayton, 1983). The overlying Devils Washbasin basalt, which he reported as intercalated with andesites of nearby Tieton Peak, yielded a stratigraphically inconsistent K/Ar age of  $3.80 \pm 0.31$  Ma. The normal magnetic polarity of the Devils Washbasin basalts and Tieton Peak andesites suggested to Clayton (1983) that these eruptions took place during the late Gauss chron, between 3.2 and 2.6 Ma. He concluded that a large composite volcano, with a total eruptive volume of at least 60 km<sup>3</sup> (comparable to presentday Mount Hood), was active between ca. 3.2 and 1.0 Ma (based on an unpublished K/Ar age of  $1.0 \pm 0.1$  Ma for Tieton andesite reported by Swanson, 1978).

USGS geologist Don Swanson began working with Clayton in 1981 as part of a multidecadal mapping campaign of the southern Washington Cascades. Products of this work include a preliminary geologic map and open-file report on the Goat Rocks Wilderness (Swanson and Clayton, 1983), two 7.5 min quadrangle maps and open-file reports (Hamilton Buttes and Packwood Lake quadrangles; Swanson, 1996a, 1996b), a nearly complete Old Snowy Mountain quadrangle map, and additional notes and mapping from adjacent Walupt Lake, Pinegrass Ridge, and Jennies Butte quadrangles.

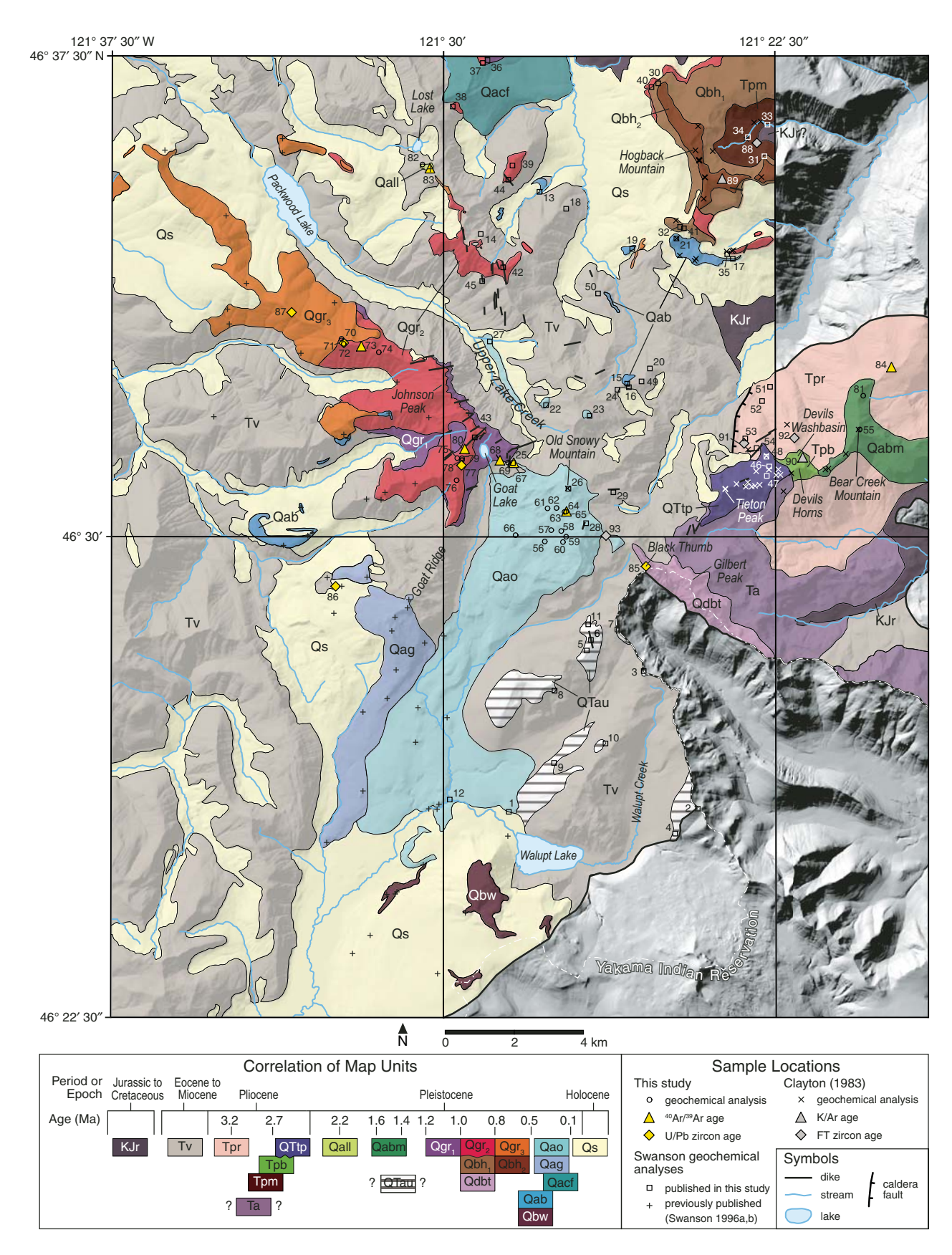


Figure 2 (Continued on facing page).

# Map unit descriptions

#### SURFICIAL DEPOSITS

Qs: Quaternary surficial deposits (Pleistocene to Holocene)—
Undifferentiated alluvium, colluvium, alluvial fan deposits, and landslide deposits, plus glacial deposits of Evans Creek and possibly Hayden Creek (MIS 6) age.

#### **OLD SNOWY MOUNTAIN STAGE**

- Qacf: Andesite of Clear Fork Cowlitz River (Pleistocene)—Gray, fine-grained, sparsely hornblende-phyric andesite flow erupted from vent on ridge just north of Coyote Lake (northern margin of map; small lake not shown). Flowed along ancestral Clear Fork Cowlitz River and ponded to form thick, strikingly columnar outcrop visible from Palisades Viewpoint on Highway 12. Occupies U-shaped valley probably carved by glacier of Hayden Creek age.
- Qao: Andesite of Old Snowy Mountain (Pleistocene)—Light gray, sparsely and finely hornblende-two pyroxene-plagioclase-phyric andesite flows erupted from Old Snowy Mountain-Ives Peak area. Typically fine-grained and pilotaxitic. Glomerocrysts of plagioclase and one or two pyroxenes are common. For simplicity, some overlying deposits of Evans Creek Drift are not shown on map.
- Qag: Andesite of Goat Ridge (Pleistocene)—Sparsely to moderately but finely two-pyroxene-plagioclase andesite on south end of Goat Ridge. Some flows are hornblende-bearing. Also includes minor dacite and rhyolite flows (units Qdg and Qrg of Swanson, 1996b). Erupted from southern crest of Goat Ridge, but glaciation has removed all trace of cones. For simplicity, some overlying deposits of Evans Creek Drift are not shown on map.
- Qab: Andesite of Brunhes Chron (Pleistocene)—Undifferentiated latestage andesites cropping out west-southwest, north, northeast, and east of Upper Lake Creek basin. Plugs and perched intracanyon flows, most amphibole-bearing. Includes Swanson's (1996a, 1996b) map units Qdj and Qgrh. Mostly normal magnetic polarity, but a few reversed; most are likely of Brunhes age, postdating unit Qgr<sub>3</sub>.
- Qbw: Basalt of Walupt Lake volcano (Pleistocene)—Hyaloclastic deposits of bedded sideromelane sand containing blocks of glassy olivine-bearing basalt, and hackly-jointed pillow-like masses of quenched basalt. Part of a large subglacial volcano (tuya) recognized by Hammond (1980). For simplicity, mapped extent also includes nearby outcrops of other young basaltic andesites (Qbt and Qba of Swanson, 1996a).

## LAKE CREEK STAGE

- Qgr<sub>3</sub>: Upper normally magnetized lava flows of Lake Creek volcano (Pleistocene)—More than 450 m of dominantly vitrophyric, cognateinclusion-bearing andesite and dacite flows filling canyons incised into older units, including older flows from Lake Creek Volcano. Flows are older than Hayden Creek age, following paleovalleys but not modern valleys.
- Qbh<sub>2</sub>: Normally magnetized basalt of Hogback Mountain (Pleistocene)—Thin flows of basalt, often olivine-bearing, capping and erupted from Hogback Mountain shield volcano. Overlies unit Ohb.
- Qgr₂: Reversely magnetized lava flows of Lake Creek volcano (Pleistocene)—Valley-filling flows totaling more than 500 m thick, dominantly vitrophyric, inclusion-bearing, and, except for reversed magnetic polarity, indistinguishable physically and chemically from older and younger flows from Lake Creek volcano.
- Qbh<sub>1</sub>: Reversely magnetized basalt of Hogback Mountain (Pleistocene)—Thin flows of basalt, often olivine-bearing, erupted from Hogback Mountain shield volcano and located stratigraphically between units Tpm and Qbh<sub>2</sub>. Lower flows in section are interbedded with reversely magnetized andesites probably from Lake Creek volcano.
- Qdbt: Dacite of Black Thumb (Pleistocene)—Thick flow/coulee of dacite lava erupted from a vent at or near Black Thumb, capping the ridge northeast of Klickitat River headwaters that includes Gilbert Peak. Note: boundary of mapped area coincides with contact for this unit.
- Qgr<sub>1</sub>: Lower normally magnetized lava flows of Lake Creek volcano (Pleistocene)—Valley-filling vitrophyric andesite and dacite flows and laharic breccia erosionally overlying Tertiary rocks. Occurs on ridges above Upper Lake Creek basin; Goat Lake cirque is eroded into this unit.

#### **BEAR CREEK MOUNTAIN STAGE**

Qabm: Andesite of Bear Creek Mountain (Pleistocene)—Plagioclaseand pyroxene-phyric andesite lava flows capping and flanking the east side of Bear Creek Mountain. Some flows contain olivine phenocrysts. Included and not distinguished on map are zones of dikes and agglomerate inferred to be vents for Tieton andesite flows (see Gusey et al., this volume, for details).

#### STAGE UNCERTAIN

- Qall: Andesite of Lost Lake (Pleistocene)—Reversely magnetized, isolated ridge-capping andesite flow remnants ~0.5 km southeast of Lost Lake. Upper flow is 2.26 ± 0.01 Ma. Vent location uncertain.
- QTau: Undifferentiated andesites (Pliocene and/or Pleistocene)—
  Andesitic to dacitic lava flows, dikes, plugs, and lahar deposits in
  Walupt Lake quadrangle of uncertain age. Probably older than Old
  Snowy Mountain stage, given deeper erosion. Includes rocks of both
  normal and reversed magnetic polarity.
- Ta: Andesite of Conrad Creek (Pliocene)—Heavily hydrothermally altered (bleached or greenish and often pyrite-bearing) andesitic lava flows or intrusions, outcropping beneath unit QTtp near the headwaters of Conrad Creek.

#### **TIETON PEAK STAGE**

- QTtp: Andesite of Tieton Peak (Pliocene and maybe Pleistocene)—
  Andesite, basaltic andesite, dacite, trachyte, and rhyolite lava flows, or possibly shallow intrusions, and pyroclastic deposits overlying unit Tpr and reportedly intercalated with unit Tpb (Clayton, 1983). The uppermost flows of andesite and dacite were initially mapped as unit Qgr<sub>1</sub>, (Swanson, 2017 written commun.), but we infer the vent to be Tieton Peak.
- Tpb: Basalt of Devils Washbasin (Pliocene)—Thin flows, bedded pyroclastic rocks, and narrow dikes of olivine basalt erupted from a vent near Devils Washbasin and comprising the spires of Devils Horns. Interbedded with pyroxene andesite flows low in unit QTtp and overlies unit Tpr. Normal magnetic polarity suggests Gauss chron, and <sup>40</sup>Ari<sup>39</sup>Ar age for a basalt flow northeast of Bear Creek Mountain, interpreted to be from this unit, is 2.78 ± 0.01 Ma.
- Tpm: Basalt and andesite of Miriam Creek (Pliocene)—Basaltic and andesitic lava flows of normal magnetic polarity underlying unit Qbh<sub>1</sub> east of Hogback Mountain. Includes the basalt of Miriam Creek (probably Pliocene but possibly Eocene; Swanson, 2017, written commun.), and overlying hornblende andesite of Miriam Lake. A zircon FT age of 3.1 ± 0.3 Ma was determined by Clayton (1983) for tephra between basalt flows midway up this section.

#### **DEVILS HORNS CALDERA**

Tpr: Rhyolite of Devils Horns (Pliocene)—Thick deposits of domes, ashflow tuff, air-fall tuff, and breccia of high-silica rhyolite beneath Devils Horns. Probably related to caldera-forming eruption (note caldera fault mapped north of Tieton Peak). Zircon FT ages ca. 3.2 Ma (Clayton, 1983).

## BASEMENT

- Tv: Undifferentiated Tertiary intrusive rocks and volcanic deposits (Eocene to Miocene)—Plutons, plugs, dikes, lava flows, and volcaniclastic and epiclastic rocks of mafic to silicic composition. Some units possibly related to the Ohanapecosh Formation (Eocene and Oligocene).
- KJr: Russell Ranch Formation (Jurassic to Cretaceous)—Graywacke, argillite, and less abundant basaltic flows, most of which are pillowed. Sheared in most places. Most flows metamorphosed to greenstone.

Figure 2 (*Continued*). Generalized geologic map of the Goat Rocks volcanic complex. Mapping and unit descriptions are compiled and modified from Swanson (1996a, 1996b) and Swanson and Clayton (1983). Numbered sample locations correspond to numbered geochemical analyses presented in Table 2 and Table DR2 (see text footnote 1). The color scheme used on this map is also adopted for Figures 6, 7, 8, and 9. FT—fission track; MIS—marine oxygen isotope stage.

In their 1983 report, Swanson and Clayton described numerous dikes crosscutting lava flows near Johnson Peak and Goat Lake, and they postulated that these are the remnants of a radial dike swarm at the center of a major composite volcano, now deeply eviscerated to form the valley occupied by Upper Lake Creek (Fig. 2). Additional geologic mapping by Swanson (1996a, 1996b) detailed a stratigraphic sequence of normalreversed-normal in the pyroxene andesites near and west of Johnson Peak, indicating that this vent was active through multiple magnetic reversals, likely recording the Brunhes-Matuyama transition. In addition, Swanson (1996a, 1996b) reported andesite (±dacite > rhyolite) lava flows that postdate this activity and occupy deep glacial valleys like those exposed along Upper Lake Creek (Fig. 2). These include the andesites of Old Snowy Mountain, Goat Ridge, and Clear Fork Cowlitz River. Swanson (1996a, 1996b) proposed that these valleys were deepened by the glaciers that deposited Hayden Creek Drift in nearby regions, for which the age has been variably estimated to be between 300 ka and 60 ka (Colman and Pierce, 1981; Crandell, 1987; Dethier, 1988; Evarts et al., 2003).

Gusey et al. (this volume) concluded that the Tieton andesite includes two channelized lava flows of enormous length; one ~74 km long and dated at  $1.64 \pm 0.07$  Ma, and the other ~52 km long with an age of  $1.39 \pm 0.10$  Ma ( $^{40}$ Ar/ $^{39}$ Ar ages in Hammond, 2017). The source of the Tieton andesite is Bear Creek Mountain (Gusey et al., this volume), not Black Thumb as proposed by Ellingson (1968).

# **Extent of the Goat Rocks Volcanic Complex**

The broadly andesitic vents of the Goat Rocks volcanic complex lie within an ~200 km² ellipsoidal area (Fig. 1). We include in the Goat Rocks volcanic complex: (1) an inferred vent at Tieton Peak (Clayton, 1983); (2) Bear Creek Mountain, source of the Tieton andesites (Gusey et al., this volume); (3) the region of dikes that define the center of Lake Creek volcano (Swanson and Clayton, 1983; Swanson, 1996b); (4) the Old Snowy Mountain area, where there are dikes and shallow intrusions (Swanson and Clayton, 1983); (5) late-stage andesitic to rhyolitic vents at Goat Ridge and Coyote Lake (Swanson, 1996a, 1996b); (6) Hogback Mountain, a possible source of early andesites (part of map unit Tpm, Fig. 2) underlying younger basalts (Clayton, 1983); and (7) Black Thumb, a dacite source near Gilbert Peak (Fig. 2; Ellingson, 1968; Clayton, 1983).

Peripheral mafic volcanoes help to define the extent of the Goat Rocks volcanic complex. The Devils Washbasin basaltic volcano (Fig. 2) marks the eastern boundary at the time of the earliest activity at Goat Rocks, although andesitic volcanism later expanded eastward. The dominantly basaltic Hogback Mountain volcano defines a northeastern boundary. The Walupt Lake basaltic tuya (subglacial volcano, unit Qbw, Fig. 2; Swanson, 1996a) marks the southern limit to Goat Rocks during the last stage of activity. Andesitic to dacitic vents to the north of Hogback Mountain (Fig. 1) are not considered to be a part of the Goat Rocks

volcanic complex, because they lie beyond the "shadow zone" (Walker, 2000) defined by these mafic volcanoes.

# **Four Volcanic Stages**

The Goat Rocks volcanic complex was constructed in four major eruptive stages. From oldest to youngest, we call these: Tieton Peak stage, Bear Creek Mountain stage, Lake Creek stage, and Old Snowy Mountain stage. We define these stages based on the chronologic sequence inferred from mapping and paleomagnetic measurements by previous authors (Clayton, 1980, 1983; Swanson and Clayton, 1983; Swanson, 1996a, 1996b) and recent work by Gusey et al. (this volume) that identified Bear Creek Mountain as a distinct vent. Below, we summarize the vents and map units that comprise each eruptive stage.

## Tieton Peak Stage

Tieton Peak stage marks the onset of andesitic volcanism at Goat Rocks, which was centered near Tieton Peak at the margin of the inferred Devils Horns caldera (Fig. 2; Clayton, 1983). Present-day Tieton Peak is built of a sequence of lava flows or possibly shallow intrusions (Judy Fierstein, 2017, personal commun.) ranging from basaltic andesite to rhyolite (map unit QTtp, Fig. 2). We caution that Tieton Peak is not the Miocene feature that Swanson (1966) described as Tieton Volcano, nor the source of the Tieton andesite flows.

Andesitic lava flows from Tieton Peak are reportedly intercalated with basaltic lava flows erupted from nearby Devils Washbasin volcano (Clayton, 1983; Fig. 2). The remains of Devils Washbasin volcano consist of basaltic dikes crosscutting basaltic lava flows and intercalated scoriaceous pyroclastic deposits (Clayton, 1983). Lava flows or intrusive rocks to the south of Tieton Peak (map unit Ta, Fig. 2) are heavily altered, commonly bleached or greenish in color, and mineralized with pyrite, suggesting near-vent hydrothermal alteration (Swanson, 2017, written commun.). Whether these altered rocks of unit Ta are an older stage of the Tieton Peak (QTtp) eruptive sequence or predate the Goat Rocks system remains to be determined.

## Bear Creek Mountain Stage

Volcanism of the Bear Creek Mountain stage was focused a few kilometers east of Tieton Peak at Bear Creek Mountain, which is built of two-pyroxene andesite lava flows and breccias that are crosscut by dikes and plugs (map unit Qabm, Fig. 2; Gusey et al., this volume). Gusey et al. (this volume) identified Bear Creek Mountain as the source of the two far-traveled Tieton andesite flows, as well as proximal lavas. The Bear Creek Mountain lava flows are reversely magnetized, and recent age determinations of the Tieton andesite flows confirm emplacement during the Matuyama chron (Hammond, 2017).

# Lake Creek Stage

Following the eruptions of Bear Creek Mountain, the primary locus of Goat Rocks volcanism moved about 12 km west

to the Lake Creek volcano. The location of this volcano can be inferred from the ridge-forming sections of andesitic to dacitic lava flows that dip radially away from the basin of Upper Lake Creek and are cut by a radial array of andesitic to dacitic dikes (map units Qgr<sub>1</sub>, Qgr<sub>2</sub>, and Qgr<sub>2</sub>, Fig. 2; Swanson, 1996b). Paleovalley-filling sections of lava flows can be thicker than 500 m and extend as far as 12 km to the northwest and northeast (Swanson, 1996b, and 2017, written commun). At Hogback Mountain, andesite to dacite lavas of Lake Creek volcano are intercalated with and capped by basaltic lava flows younger than ca. 0.9 Ma (Sisson and Calvert, 2017, written commun.; Swanson, 2017, written commun.). The volcanic products of the Lake Creek stage are deeply incised and glacially sculpted at high elevation. Geochronology (discussed below) indicates that the dacite plug or coulée of Black Thumb (unit Qdbt, Fig. 2) was also erupted during this stage.

#### Old Snowy Mountain Stage

After the Lake Creek stage and a period of deep glacial erosion, volcanism of the Old Snowy Mountain stage commenced. The most voluminous eruptions occurred from vents near Old Snowy Mountain and Ives Peak (Swanson and Clayton, 1983; Swanson, 1996a, 1996b). Other andesitic eruptions occurred at the southern end of Goat Ridge (unit Qag, Fig. 2), and from a vent at Coyote Lake that fed the Clear Fork andesite (unit Qacf, Fig. 2; Swanson, 1996b). Young andesitic to dacitic flows from minor vents or of uncertain source are also assigned to this stage (unit Qab). Lava flows from Old Snowy Mountain are present low in the valley of Upper Lake Creek, attesting to the deep erosion between the Lake Creek and Old Snowy Mountain stages. Old Snowy Mountain stage lavas are mainly andesite, with lesser dacite, and extending to rhyolite. Amphibole is a common component of the typical two-pyroxene mafic assemblage, and, in some cases, it is the dominant mafic mineral.

# **METHODS**

# Mapping and Sample Collection

Petrographic descriptions and chemical analyses for 54 Pliocene to Pleistocene volcanic samples were provided by Don Swanson. Swanson collected these and other samples between 1981 and 1996 in Packwood Lake, Old Snowy Mountain, Pinegrass Ridge, and Walupt Lake quadrangles and mapped these regions with the aid of a portable fluxgate magnetometer.

In 2015, 2016, and 2017, we revisited the areas mapped by Swanson in the above quadrangles and the Hamilton Buttes quadrangle. In 2017, we used a portable fluxgate magnetometer (MEDA  $\mu$ MAG-01) at selected outcrops, taking at least three readings per site to confirm whether the rock was magnetically normal or reversed. If the reading induced by the rock was indistinguishable from small movements of the handheld sensor probe during measurement, we assigned an indeterminate magnetic polarity for the outcrop.

We collected a total of 143 rock samples from the Goat Rocks volcanic complex. Thirteen of these samples were dated by either the <sup>40</sup>Ar/<sup>39</sup>Ar or U/Pb methods, and 30 samples were geochemically analyzed (locations in Table 1 and Fig. 2; see also Table DR2<sup>1</sup>).

# **Analytical Methods**

## <sup>40</sup>Ar/<sup>39</sup>Ar Geochronology

Samples for 40Ar/39Ar dating were prepared and analyzed at the Oregon State University Argon Geochronology Laboratory. Samples were crushed and sieved to 125–355 µm, washed, and then passed through a Frantz magnetic separator to isolate groundmass from phenocrysts. All groundmass, plagioclase, and amphibole separates were cleaned by a rigorous acid leaching procedure involving 1 h each of 1 N HCl, 6 N HCl, 1 N HNO<sub>3</sub>, 3 N HNO<sub>3</sub>, and triple-distilled H<sub>2</sub>O. Plagioclase separates were additionally treated with 5% HF for 8 min to remove adhering glass and/or volcanic matrix, and cleaned with triple-distilled water for an additional 1 h in an ultrasonic bath. High-purity separates were handpicked under a binocular microscope, with particular attention paid to removing plagioclase crystals with visible inclusions. Ten to 50 mg aliquots of each separate were encapsulated in aluminum foil and loaded with the Fish Canyon Tuff sanidine flux monitor (FCT-NM; age  $28.201 \pm 0.023$  Ma [ $1\sigma$ ]; Kuiper et al., 2008) and vacuum-sealed in quartz vials. Sample heights were determined using a Vernier caliper. The samples and flux monitors were irradiated for 6 h in three separate irradiations (15-OSU-06, 17-OSU-01, 17-OSU-06) in the cadmium-lined in-core irradiation tube (CLICIT) of the TRIGA (Training, Research, Isotopes, General Atomics) nuclear reactor at Oregon State University.

The 40Ar/39Ar ages were determined by incremental heating using a CO<sub>2</sub> laser and analyzed using a multicollector ARGUS-VI mass spectrometer at the Argon Geochronology Laboratory at Oregon State University. Ages were calculated using the decay constant of  $5.530 \pm 0.097 \times 10^{-10} \text{ yr}^{-1} (2\sigma)$  as reported by Min et al. (2000); for other constants, refer to Table 2 in Koppers et al. (2003) or Supplementary Information DR1 (see footnote 1). Plateau and isochron ages were calculated as weighted mean ages with  $1/\sigma^2$  as the weighting factor (Taylor, 1997) and as YORK2 least-square fits with correlated errors (York, 1968) using the ArArCALC v2.6.2 software from Koppers (2002). All <sup>40</sup>Ar/<sup>39</sup>Ar ages are reported at 2σ uncertainty (Table 1; Fig. 3; Supplementary Information DR1). When the inverse isochron for a sample suggested an initial <sup>40</sup>Ar/<sup>36</sup>Ar ratio that was not within 2σ error of the standard value for air (295.5), we used the data-defined <sup>40</sup>Ar/<sup>36</sup>Ar(i) value to recalculate the plateau age (propagating the error on the <sup>40</sup>Ar/<sup>36</sup>Ar[i] through the calculation). Ages

<sup>&</sup>lt;sup>1</sup>GSA Data Repository Item 2018236, Age and compositional data for Goat Rocks volcanic complex, is available at www.geosociety.org/datarepository/2018/, or on request from editing@geosociety.org or Documents Secretary, GSA, P.O. Box 9140, Boulder, CO 80301-9140, USA.

Sample ID*	Map no. <sup>†</sup>	Map unit§	Location*	tion#	Magnetic	Age ± 2o error	Phase	Dating	Details##	Age interpretation	Keterence***
! <u>-</u>	-		Longitude (°W)	Latitude (°N)	polarity**	(ka or Ma) <sup>††</sup>	analyzed§§	technique			
Old Snowy M	Old Snowy Mountain stage GR17-78 N.A.	2 Qacf	121.5480	46.6791	z	107 ± 5 (ka)	Zm	U/Pb	Surfaces $(n = 4)$ and	Youngest zircon population	This study
									interiors $(n = 5)$ , MSWD = 2.22		
GR16-25	65	Оао	121.4549	46.5065	z	217 ± 5	В	40Ar/39Ar	Plateau, 52% <sup>39</sup> Ar(k), MSWD = 1.13	Groundmass crystallization	This study
GR16-38	29	Оао	121.4747	46.5188	z	440 ± 3	В	40Ar/39Ar	Plateau, 52% 39Ar(k), MSWD = 1.05	Groundmass crystallization	This study
						453 ± 8	Zrn	U/Pb	Interiors $(n = 9)$ , MSWD = 7.22	Youngest zircon population	This study
GR17-71	98	Qag	121.5400	46.4866	z	443±10	Zrn	U/Pb	Surfaces $(n = 4)$ and low-Y interiors $(n = 5)$ , MSWD = 1.19	Youngest zircon population	This study
Lake Creek stage GR15-04	<u>tage</u> 73	Qgr <sub>2</sub>	121.5322	46.5492	Œ	593 ± 4	Gm	40Ar/89Ar	Plateau, 60% 39Ar(k), MSWD = 1.23	Groundmass crystallization	This study
						626 ± 77	Am	40Ar/39Ar	mSWD = 1.23 Plateau, 96% %Ar(k), MSWD = 1.70	Amphibole crystallization	This study
GR17-75 (GR15-02)	71	$Agr_2$	121.5388	46.5501	Œ	600 ± 29	Zrn	U/Pb	Surfaces $(n = 9)$ , MSWD = 0.36	Youngest zircon population	This study
GR17-72A	87	Qgr <sub>3</sub>	121.5572	46.5574	z	742 ± 17	Zrn	U/Pb	Interiors $(n = 11)$ , MSWD = 1.07	Youngest zircon population	This study
GR17-47A	82	Qdbt	121.4241	46.4916	Œ	817 ±24	Zrn	U/Pb	Surfaces $(n = 5)$ and interiors $(n = 9)$ , MSWD = 0.67	Youngest zircon population	This study
GR16-34	80	$Agr_2$	121.4932	46.5224	Œ	820 ± 3	Gm	40Ar/89Ar	Plateau, 54% **Ar(k), MSWD = 1.37	Groundmass crystallization	This study
						874 ± 30	Zrn	U/Pb	Interiors $(n=6)$ , MSWD = 1.3	Youngest zircon population	This study
08WP1019 GR16-30	Z.A.	Qbh <sub>1</sub> ## Qgr <sub>2</sub>	121.4297 121.4944	46.6483 46.5184	Ä. Ö. R	891 ± 7 987 ± 57	Gm Zm	<sup>40</sup> Ar/ <sup>39</sup> Ar U/Pb	Plateau Interiors $(n=9)$ ,	Youngest zircon population	1 This study
N.G. GR16-36	89 89	Un. <sup>§§§§</sup> Qgr <sub>1</sub>	121.4390 121.4799	46.4990 46.5198	a. Z	1.11 ± 0.09 (Ma) 1.11 ± 0.03	Zm Zm	Fission track U/Pb	<u>-</u>	Youngest zircon population	2, 3 This study
						1.11 ± 0.01	Gm	40Ar/39Ar	Total fusion	Groundmass	This study
						1.13 ± 0.01	₫	40Ar/39Ar	Plateau, 80% 39Ar(k),	Plagioclase cooling age	This study
HM-SP-1	08	440	000	1	:				INISWD = 1.20		

TABLE 1. AGES OF PLIOCENE TO PLEISTOCENE VOLCANIC DEPOSITS NEAR GOAT ROCKS VOLCANIC COMPLEX (Continued)

	Ξ.	טבר ו. ממבט		10111	OOLINE VOEV	ANIO DEI OGILO	מס ועשוי		INDEED IN AGES OF TELEGOEINE TO LEFE TO SECOND OF THE TOTAL GOAL THOUGH SOUTH THE TELEGOEINE TO THE TOTAL GOAL THOUGH THE TELEGOEINE THE TOTAL GOAL THOUGH THE THE TOTAL GOAL THOUGH THE TOTAL GOAL THOUGH THE TOTAL GOAL THOUGH THE TOTAL GOAL THOUGH THE THE TOTAL GOAL THOUGH THE TOTAL GOAL THE THE TOTAL GOAL THOUGH THE THE TOTAL GOAL THE TOTAL GOAL THE THE THE TOTAL GOAL THE TOTAL GOAL THE TOTAL GOAL THE TOTAL GOAL TH	(Columbed)	
Sample ID*	Map no.⁺	Map no.⁺ Map unit <sup>§</sup>	Location#	"ion#	Magnetic	Age ± 2o error	Phase	Dating	Details##	Age interpretation	Reference***
			Longitude (°W)	Latitude (°N)	polarity**	(ka or Ma) <sup>#</sup>	analyzed <sup>§§</sup>	technique			
Bear Creek №	Bear Creek Mountain stage	en.									
N.G.	Z.A.	Qta,	121.1833	46.6320	Œ	$1.35 \pm 0.13$	Zrn	Fission track			2, 4
07114	Z.A	Qta,	120.8169	46.7194	Œ	$1.39 \pm 0.10$	⊡	40Ar/39Ar			2
04162	Z.A	Qta <sub>,</sub>	121.1515	46.6786	Œ	$1.64 \pm 0.07$	Gm	40Ar/39Ar			2
Tieton Peak stage	stage										
GR16-07	84	Трр	121.3324	46.5439	z	2.68 ± 0.01	Gm	<sup>40</sup> Ar/ <sup>39</sup> Ar	Plateau, 76% 39Ar(k), MSWD - 0.79	Groundmass crystallization	This study
GRDH-2	06	Трь	121.3659	46.5205	z	$3.80 \pm 0.31$	WB	K/Ar			2, 3
Unassigned stage GR16-12	<u>stage</u> 83	Qall	121.5063	46.5957	œ	2.27 ± 0.01	G	40Ar/39Ar	Plateau. 66%	Groundmass	This study
									<sup>39</sup> Ar(k), MSWD = 4.23	crystallization	
						2.29 ± 0.01	⊡	<sup>40</sup> Ar/ <sup>39</sup> Ar	Plateau, 63% <sup>39</sup> Ar(k), MSWD = 1.53	Plagioclase cooling age	This study
HMMCSP-2	88	Tpm	121.3831	46.6025	z	$3.1 \pm 0.2$	Zrn	Fission track			2, 3
Pre-Goat Rocks	cks										
GRTPC-9	91	Tpr	121.3880	46.5241	N.D.	$3.17 \pm 0.16$	Zrn	Fission track			2, 3
GRDH-3	92	Tpr	121.3690	46.5255	N.D.	$3.20 \pm 0.14$	Zrn	Fission track			2, 3

Note: Plagioclase ages for samples GR15-04, GR16-07, and GR16-25 are in Supplementary Information DR1 (see text footnote 1).

\*N.G. -no sample ID given.

'IN.A.—not applicable (location is outside of Fig. 2 boundary). §Map units as in Figure 2, except for Qta, and Qta<sub>2</sub> (older and younger Tieton andesite flows; Gusey et al., this volume).

<sup>\*</sup>Longitude and latitude measured by global positioning system (GPS; coordinate reference system World Geodetic System 1984 [WGS84]; this study, refs. 1, 4, 5), or approximated from sample locations in Clayton (1980).

<sup>\*\*</sup>Measured by portable fluxgate magnetometer or inferred from map units by Swanson (1996a, 1996b). N—normal, R—reversed, N.D.—not determined (or no magnetic signal).
#\*Monitalic font—age from this study; italic font—age from a previous study (see Reference column), bold font—preferred eruption ages included on Figure 5, nonbold font—age that is not interpreted as the eruption age (e.g., phenocryst age older than groundmass from the same sample), or one that is considered a less reliable age (e.g., previously published age that does not agree with stratigraphic relations).

<sup>§</sup>Zrn—zircon, Gm—groundmass, PI—plagioclase, Am—amphibole, WR—whole-rock.

<sup>\*\*</sup>For zircon ages, n—number of spot analyses on crystal surfaces or polished interiors that were included in the weighted mean age. MSWD—mean square of weighted deviates. \*\*\*1—Sisson and Calvert (2017, written commun.); 2—Clayton (1983); 3—Clayton (1980); 4—Gusey et al. (this volume); 5—Hammond (2017)

tttMap unit is interpreted from age, but not confirmed. 889Un. – unassigned. Sample was identified as part of the Cispus Pass pluton, but mapping of this pluton is unresolved.

TABLE 2. REPRESENTATIVE X-RAY FLUORESCENCE (XRF) MAJOR- AND TRACE-ELEMENT BULK COMPOSITIONS OF

Map no.	:	15	19	27	30	31	33	34	36	39	40	42	46	47	48	51
Sample	ID:	81-35	96-17	96-23	96-27	96-55	96-29	96-54	82-83	82-105	96-28	81-25	96-52	96-51	96-50	96-45
Map uni	t <sup>†</sup> :	Qab	Qab	Qao	Qbh1	Qbh1	Tpm	Tpm	Qgr1	Qgr2	Qgr2	Qgr3	QTtp	QTtp	QTtp	Tpr
Rock typ	oe§:	pl	lf	lf	lf	pl	lf	lf	If	If	If	dk	lf	lf	lf	fr
Classific	ation#:	rhy	rhyodac	and	bas	gab	bas	bas and	dac	and	and	dac	rhyodac	rhyodac	and	rhy
Mineral assembl	lage**:	NR	am, pl	px, pl, oxyhbl	ol	cpx, opx	ol	ol	NR	NR	pl, cpx, opx	NR	pl, cpx, am	pl, cpx, am	oxyhbl(?)	pl
<u>Major-el</u>			n, normalize	ed volatile-	free to 10	0 percen	t (wt%)									
	Uncerta (%) <sup>††</sup>	ainty														
SiO <sub>2</sub>	0.19	71.95	70.31	60.31	51.34	58.58	49.91	55.33	66.30	61.25	62.06	66.55	68.65	69.91	61.36	75.70
$Al_2O_3$	0.50	14.55	14.88	17.09	15.72	17.53	16.14	16.59	15.67	16.07	16.20	15.41	16.09	14.81	17.21	14.07
TiO <sub>2</sub>	0.92	0.39	0.49	0.95	1.26	0.85	1.30	0.95	0.72	1.10	1.12	0.67	0.66	0.37	0.79	0.03
FeO*	1.17	2.61	3.14	6.22	8.82	6.44	10.41	7.57	4.32	6.11	5.76	4.19	3.60	4.29	6.25	1.32
MnO	0.68	0.05	0.06	0.10	0.15	0.11	0.16	0.13	0.07	0.10	0.09	0.07	0.04	0.03	0.09	0.05
CaO	0.69	2.34	2.80	6.13	9.36	7.18	9.78	8.73	4.05	5.53	4.77	3.95	1.96	0.80	6.13	1.56
MgO	1.33	0.64	1.09	3.34	9.00	3.98	8.16	5.66	1.83	3.08	2.84	1.85	0.26	0.05	2.78	0.39
K <sub>2</sub> O	0.71	3.13	2.84	1.46	1.11	1.37	0.75	1.19	2.79	2.61	2.84	3.05	3.67	4.28	1.51	5.05
Na <sub>2</sub> O	1.34	4.23	4.26	4.10	2.93	3.79	3.16	3.64	4.09	3.92	4.09	4.09	4.90	5.40	3.63	1.80
P <sub>2</sub> O <sub>5</sub> Unnorm	2.16	0.10 99.08	0.12 99.97	0.30 100.50	0.32 99.80	0.18 99.91	0.24 99.29	0.21 99.10	0.16 98.55	0.23 98.73	0.24 100.72	0.16 97.26	0.17 98.94	0.07 99.30	0.25 98.12	0.03 97.58
total		99.00	33.37	100.50	33.00	33.31	33.23	33.10	90.55	30.73	100.72	97.20	30.34	99.50	30.12	97.50
Trace-el	ement cor	ncentration	n (ppm)													
	Uncerta (%) <sup>††</sup>	ainty														
Ni	6.61	8	8	28	129	6	104	21	13	17	27	13	5	5	8	13
Cr	5.05	7	6	52	368	35	310	129	17	43	51	19	3	0	18	0
Sc	5.34	5	8	17	30	24	28	28	12	14	15	8	4	4	15	8
V	2.60	35	55	121	187	166	207	178	89	136	122	78	39	23	80	4
Ba	1.57	637	531	443	442	297	218	249	499	431	511	505	697	815	341	430
Rb	2.71	96	89	29	20	20	14	16	89	83	86	98	90	104	22	119
Sr	0.73	262	276	579	550	623	418	773	295	347	348	284	215	112	763	84
Zr	0.90	148	153	198	153	141	117	135	198	269	296	222	376	466	138	56
Y	3.01	17	16	19	22	16	24	19	24	27	22	23	33	45	19	27
Nb	5.23	11	11	14	12	6	12	5	15	19	22	15	33	45	7	14
Ga	3.82	18	19	21	17	20	20	18	19	21	20	19	24	26	25	24
Cu	3.63	10	27	45	22	30	42	30	16	16	29	11	0	7	18	6
Zn	1.98	41	48	84	77	69	80	70	56	65	61	55	84	91	71	53
Pb	8.71 8.71	11 26	9 32	5 19	1 27	4 17	0 5	0 23	10 30	4 25	5 44	8 21	13 40	10 52	3 10	17 16
La Ce	6.48	26 54	32 48	19 49	27 58	40	5 39	23 39	65	25 73	44 74	21 57	40 77	52 97	50	31
Th	10.34	5 <del>4</del> 12	46 11	49	56 6	40 2	39 4	39	10	73 11	8	10	12	97 7	3	6
Nd	6.94	14	1.1	+	O	_	4	3	10	1.1	J	10	14	,	3	U

Note: Additional XRF analyses, location data for all samples, and inductively coupled plasma-mass spectrometry (ICP-MS) data for samples with prefix GR are in Table DR2 (see text footnote 1).

<sup>\*</sup>Asterisk in GR16-08\* and GR16-09\* is part of sample name. Note that sample GR15-02 is from the same outcrop as GR17-75 (age presented in Table 1).

<sup>†</sup>Map units as in Figure 2, except unit Qta, (Gusey et al., this volume) not shown in Figure 2. §If—lava flow, dk—dike, pl—plug, fr—fragmental deposit, en—enclave separated from host lava.

<sup>\*</sup>and—andesite, bas—basalt, bas and—basaltic andesite, dac—dacite, rhy—rhyolite, rhyodac—rhyodacite.

\*\*Mineral assemblages are from Swanson (2017, written commun.), hand sample characterization, and preliminary petrography. NR—not reported, pl—plagioclase, ol—olivine, am—amphibole, opx—orthopyroxene, cpx—clinopyroxene, px—undifferentiated pyroxene, oxyhbl—oxyhornblende, gloms—glomerocrysts.

<sup>&</sup>lt;sup>††</sup>Analytical uncertainty for 2016 and 2017 analyses (samples with prefix GR) is based on the mean relative percent absolute difference (RPAD) reported for each element by Kelly (2016); see Methods section.

55	59	60	62	65	67	68	70	70	72	73	77	81	82	83	Map no.:
GR16- 09*	GR16- 19	GR16- 20	GR16- 22	GR16-25	GR16-38	GR16-36	GR15- 01B	GR15- 01C	GR15- 03	GR15-04	GR16-30	GR16-08*	GR16-10	GR16-12	Sample ID:
Qabm	Qao	Qao	Qao	Qao	Qao	Qgr1	Qgr2	Qgr2	Qgr2	Qgr2	Qgr2	Qta2	Qall	Qall	Map unit†:
lf	If	If(?)	fr	If	lf	If	en	dk	If	If	If	If	If	If	Rock type§:
and	and	and	and	dac	and	and	and	dac	and	rhyodac	dac	and	and	and	Classification#:
pl, cpx, ol	pl, cpx(?)	pl	pl	am, pl, pl-cpx gloms	pl, am, cpx, opx	pl, cpx	pl, am	pl, am, cpx-opx-pl gloms	pl, cpx	pl, am	pl, cpx	pl, cpx	pl	pl, pl-px gloms	Mineral assemblage**:
									<u>Major-</u>	element co	ncentration	n, normaliz	ed volatile-	free to 10	00 percent (wt%)
61.31	61.45	58.00	60.74		60.98	61.24	61.00	67.92	61.48		64.11	60.75	61.33	61.90	41.0
16.07	17.22	18.00	17.84		17.00	16.21	17.20	15.35	16.45		15.97	16.03	15.75	15.83	T:0
1.13	0.90	1.15	0.91		0.91	1.15	0.93	0.61	1.00		0.93	1.18	1.19	1.10	
6.18	5.86	7.07	5.86		5.72	6.25	6.06	3.92	6.03		5.20	6.45	6.14	5.81	FeO*
0.10	0.10	0.13			0.10	0.11	0.10	0.07	0.09	0.07	0.09	0.11	0.10	0.10	
5.13	6.08	7.19	6.57		6.34	5.44	5.94	3.63	5.69		4.28	5.65	5.59	5.31	CaO
3.01	2.87	3.46	3.02		3.23	2.83	3.15	1.59	2.85		2.10	3.28	3.33	3.27	14.0
2.87	1.57	1.20			1.80	2.68	1.71	2.81	2.29		3.16	2.63	2.64	2.67	N 0
3.95	3.79	3.62			3.71	3.83	3.66	3.96	3.86		3.96	3.68	3.69	3.77	
0.25	0.16	0.18	0.16		0.22	0.26	0.24	0.14	0.25		0.21	0.24	0.25	0.24	
99.51	99.35	99.44	98.16	99.36	99.11	98.36	98.97	99.27	99.30	99.48	98.55	99.05	98.45	98.38	Unnorm. total
													Trace-ele	ment con	centration (ppm)
31	16	18	19	12	26	24	29	13	21	11	16	32	28	41	Ni
51	34	33	31	21	35	39	55	19	31	19	28	63	68	63	Cr
15	15	20	16	11	16	16	16	9	17	9	11	17	16	16	Sc
117	128	167	129	91	138	121	123	69	136	64	89	146	132	121	V
465	324	270	312	334	443	461	410	544	500	544	503	424	474	477	Ba
91	33	24	34	34	49	81	38	84	66	97	103	82	70	69	Rb
352	506	515	559	506	539	387	431	289	559	274	313	362	385	401	Sr
346	139	140	137	151	159	312	184	187	206	187	347	298	292	299	Zr
28	17	21	18	15	16	27	19	18	23	18	29	28	27	26	Υ
24	7	8	7	7	10	22	12	12	12	12	21	21	20	20	Nb
19	19	20	20	21	20	20	20	17	20	18	19	20	19	20	Ga
23	42	45	45	32	35	23	20	16	28	15	23	39	28	24	Cu
70	67	74	63	68	68	70	91	55	72	54	67	70	74	72	Zn
9	7	6	6	8	6	8	17	11	8	10	9	8	10	10	Pb
31	19	17	18	17	23	30	23	28	27	26	35	32	30	30	La
68	34	33	39	36	52	72	49	48	63	49	67	59	65	63	Ce
11	5	4	4	4	7	9	6	11	9	13	12	10	8	8	Th
31.0	14.8	17.2	18.8	15.6	23.0	30.2	24.0	19.9	29.0	21.3	30.4	29.2	28.8	29.0	Nd

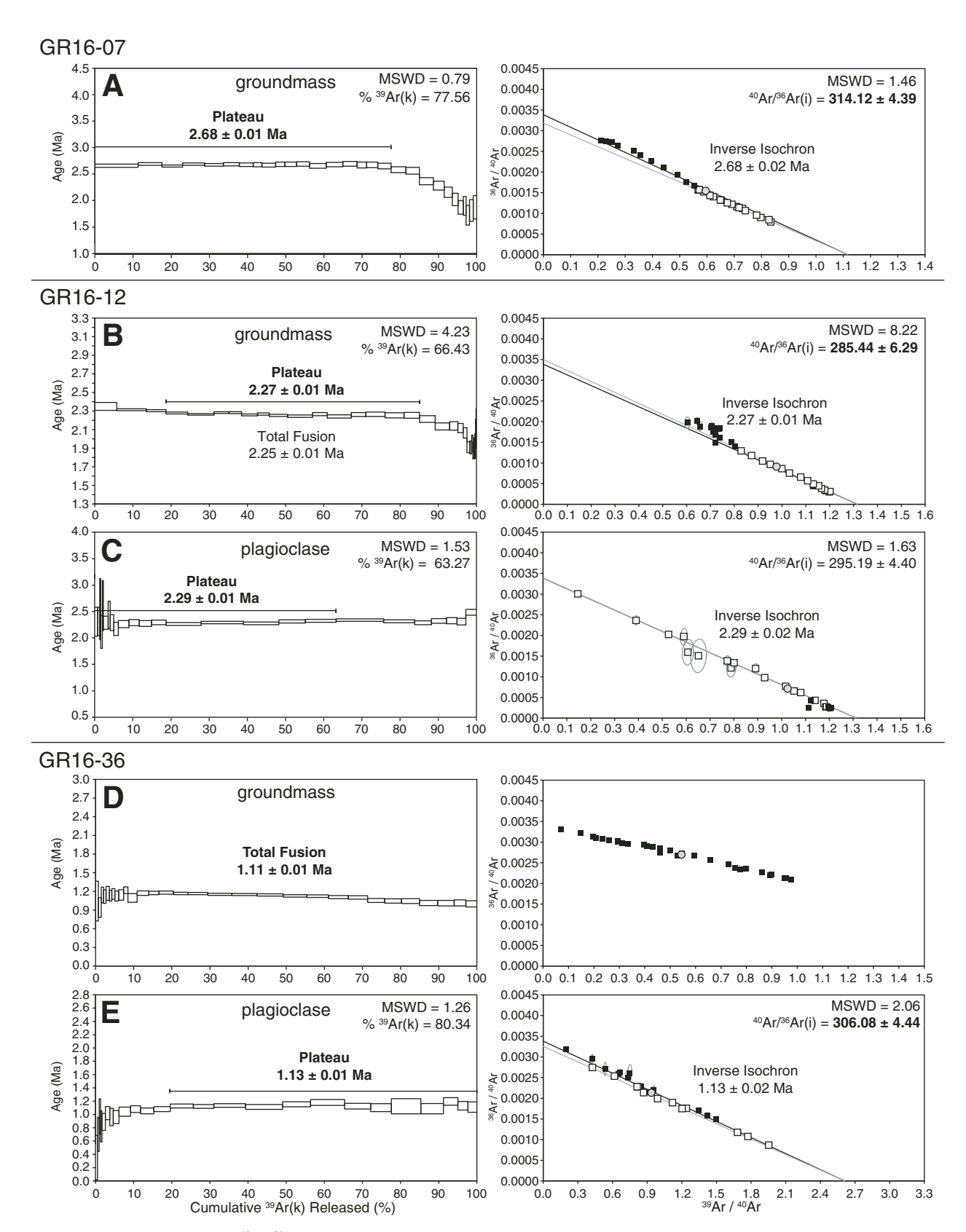


Figure 3 (*Continued on facing page*). <sup>40</sup>Ar/<sup>39</sup>Ar age spectra and inverse isochrons for seven samples from Goat Rocks volcanic complex and vicinity. The preferred age for each groundmass or mineral separate is in bold. Heating steps included in the plateau age are white boxes used to fit black and gray inverse isochrons. The black inverse isochron line is fit to the intercept value of air; the calculated intercept for the gray line is in the upper-right corner of the plot. Calculated <sup>40</sup>Ar/<sup>36</sup>Ar intercept values are shown in bold when not within error of the standard value for air (295.5) and when used in the plateau calculation. Total fusion data are indicated by gray circles with bold outlines on inverse isochron diagrams. For full data sets for each sample, see Supplementary Information DR1 (text footnote 1). MSWD—mean square of weighted deviates.

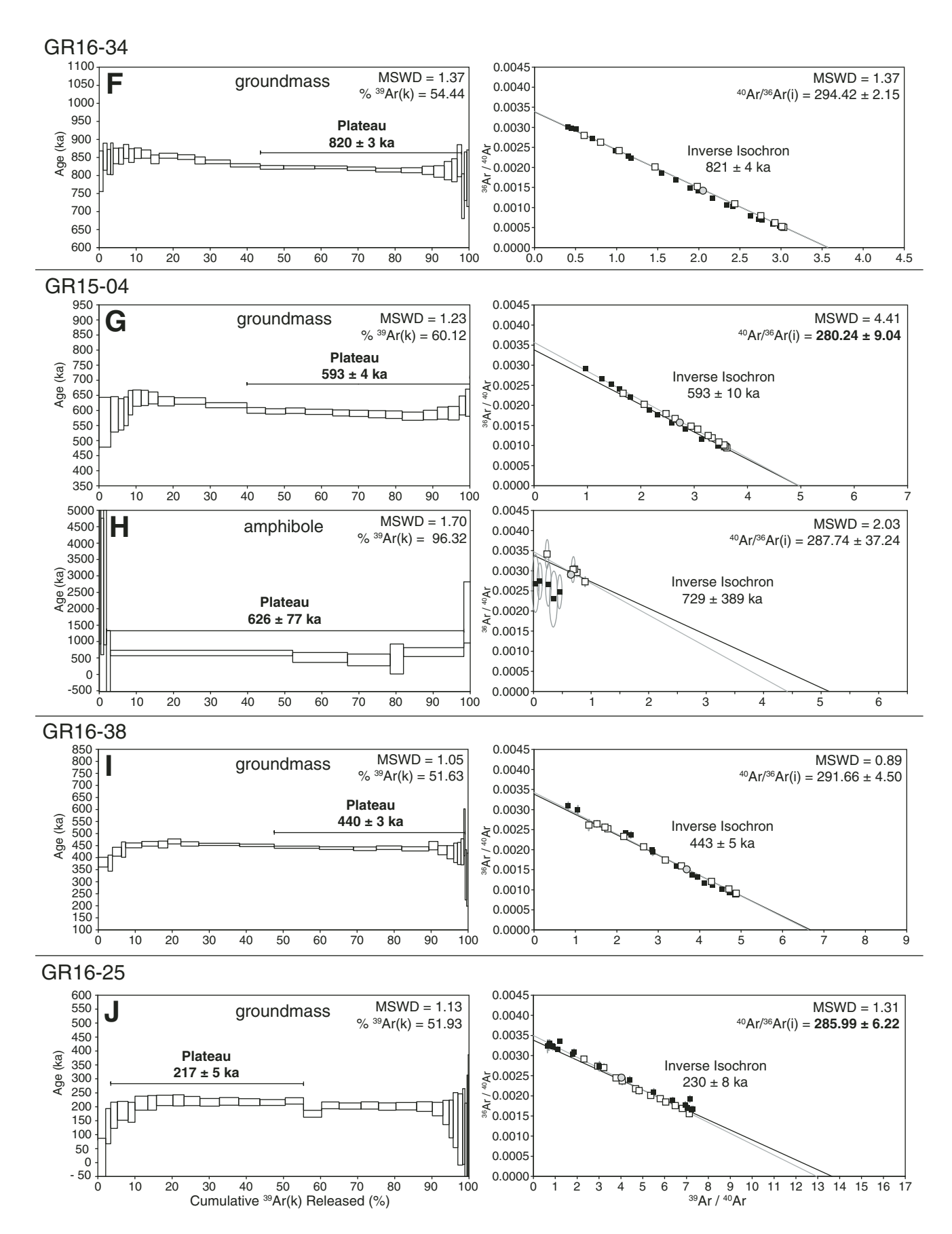


Figure 3 (Continued).

presented here contain between 52% and 96% of the cumulative <sup>39</sup>Ar released for a given sample. In this paper, we defined a plateau as three or more contiguous heating steps that represent at least 50% of the cumulative <sup>39</sup>Ar released. Each of our plateau ages has a mean square of weighted deviates (MSWD) below the 95% confidence limit as defined by Mahon (1996), except for one groundmass sample (GR16-12). All plagioclase separates yielded age spectra and inverse isochrons that suggest excess argon, probably from microscopic melt inclusions. Plagioclase separates for two samples yielded plateau ages within uncertainty of the groundmass plateau or total fusion ages, but plagioclase for three samples (GR15-04, GR16-07, GR16-25) did not yield plateau ages. Pseudo-plateaus (containing 27% to 33% of the <sup>39</sup>Ar released) for those plagioclase separates are significantly older than the groundmass ages for those samples and were not considered reliable eruption ages; however, the analytical data for those plagioclase analyses can be found in Supplementary Information DR1 (see footnote 1).

## U/Pb Geochronology

Samples for U/Pb dating were crushed and panned under running water to concentrate high-density minerals. The nonmagnetic fraction was recovered from the high-density material via a Frantz magnetic separator and examined under binocular microscope with the aid of polarizing film. Zircons were hand selected, mounted in epoxy and polished, or pressed into an indium metal mount, and then imaged using cathodoluminescence (CL) at either the Oregon State University Electron Microscopy Facility or Stanford University to identify internal zonation, cracks, or inclusions, and to guide in situ analyses.

Zircon mounts were analyzed using the sensitive highresolution ion microprobe with reverse geometry (SHRIMP-RG) at the Stanford-USGS MicroAnalysis Center (SUMAC) to obtain U/Pb ages and trace-element compositions. The spot size for individual analyses was ~25 µm in diameter and 1-2 µm deep, providing the high spatial resolution needed to avoid identifiable cracks as well as apatite and melt inclusions (Schaltegger et al., 2015). On polished mounts, spots were analyzed on individual zircons of variable appearance (size, morphology, CL brightness, zonation pattern), targeting rims, intermediate zones, and cores in efforts to survey the range of ages and compositions present in each sample. For the four samples mounted in indium, spots were analyzed on surfaces of zircons in order to determine the age of the most recent crystallization (e.g., Vazquez and Lidzbarski, 2012; Matthews et al., 2015; Coble et al., 2017).

Calculated model ages for zircon were standardized relative to Temora-2 (416.8 Ma; Black et al., 2004), which was analyzed repeatedly throughout the duration of the analytical sessions. Early-erupted Bishop Tuff zircon (EBT; Crowley et al., 2007) was analyzed as a secondary standard and yielded a weighted mean age of  $786 \pm 23$  ka (see Table DR1 for full data set [footnote 1]). This age is within  $2\sigma$  error of the isotope dilution—thermal ionization mass spectrometry (ID-TIMS) age of  $767.1 \pm 0.9$  ka by

Crowley et al. (2007) for Bishop Tuff zircon. Samples were corrected for disequilibrium of the 230Th intermediate daughter product using the method of Schärer (1984) and initial <sup>232</sup>Th/<sup>238</sup>U<sub>melt</sub> values based on new U and Th concentrations measured by inductively coupled plasma-mass spectrometry (ICP-MS; samples GR16-30 and GR16-38) or estimated at 3.0 for all other samples not yet analyzed for bulk composition. The <sup>238</sup>U/<sup>206</sup>Pb dates were corrected for common Pb using measured 207Pb/206Pb (Ireland and Williams, 2003) and assuming a <sup>207</sup>Pb/<sup>206</sup>Pb<sub>common</sub> value from Stacey and Kramers (1975). Zircon trace-element concentrations were standardized relative to sample MAD-559 (U = 3435 ppm), a homogeneous in-house zircon standard calibrated relative to MAD-green (Barth and Wooden, 2010). Individual spot ages are reported at 1σ analytical error. The youngest zircon crystallization age for each sample is interpreted as either: (1) weighted mean and  $2\sigma$  standard error of interiors of compositionally and texturally similar crystals, for samples only in polished mounts, (2) weighted mean and  $2\sigma$  standard error of crystal surfaces that define a coherent population, or (3) weighted mean and  $2\sigma$  standard error of both interior ages and surface ages, when these individual ages overlap within  $2\sigma$  uncertainty.

# Bulk X-Ray Fluorescence and ICP-MS Geochemistry

Samples collected in 2015 (prefix GR15) and 2016 (GR16) were prepared and analyzed via X-ray fluorescence (XRF) and ICP-MS at the Peter Hooper GeoAnalytical Laboratory at Washington State University. Samples for XRF analyses were prepared following the procedures of Johnson et al. (1999). The accuracy and precision of the major-element XRF analyses are as described in Johnson et al. (1999), with modifications summarized by Kelly (2016). Improved accuracy of Zr and Cr for samples analyzed since 2004 and 2007, respectively, was described by Sawlan (2018).

Uncertainty for each XRF elemental analysis is based on the relative percent absolute difference (RPAD; Eq. 1) in the measured concentration of an element for two aliquots of the same sample (Kelly, 2016).

$$RPAD = \left| (Aliquot\ 1 - Aliquot\ 2) \div \frac{(Aliquot\ 1 + Aliquot\ 2)}{2} \right| * 100. \quad (1)$$

The mean RPAD value for each element, used here as a measure of uncertainty (Table 2), combines RPAD values determined from over 250 samples and their repeat analyses (Kelly, 2016). Samples for ICP-MS were prepared and analyzed following procedures noted on the Washington State University laboratory website (Peter Hooper GeoAnalytical Laboratory, "ICP-MS Method," https://environment.wsu.edu/facilities/geoanalytical-lab/technical-notes/icp-ms-method/) and modified by Steenberg et al. (2017). Based on ~100 ICP-MS analyses of several certified reference materials (CRMs), Steenberg et al. (2017) determined the average relative percent differences from GeoReMaccepted values (http://georem.mpch-mainz.gwdg.de/), which range from 6.32% (Ho) to 1.66% (Ba), with an average of 3.37%. Samples collected by Swanson were analyzed at the

USGS laboratory in Lakewood, Colorado, or in 1996 at Washington State University.

#### **RESULTS**

#### Geochronology

Eruption and shallow intrusion of andesite and dacite lavas persisted at Goat Rocks for 2.5–2.9 m.y. (from between 3.0 and 2.6 Ma to 0.1 Ma), based on a combination of new <sup>40</sup>Ar/<sup>39</sup>Ar ages and U/Pb ages for 13 samples and 10 previous ages (Table 1), in concert with field relations and magnetic polarity measurements. The new ages constrain the Devils Washbasin basalt, Lost Lake andesite, andesites and dacites from Lake Creek volcano, Black Thumb dacite, Old Snowy Mountain andesites, Goat Ridge rhyolite, and Clear Fork andesite (for sample locations, see Table 1 and Fig. 2). Previous ages (K/Ar, zircon fission-track, and <sup>40</sup>Ar/<sup>39</sup>Ar) are from the Devils Horns rhyolite, Devils Washbasin basalt, a dacite tuff along Miriam Creek, Tieton andesite, Hogback Mountain basalt, and the Cispus Pass pluton (Table 1).

#### Tieton Peak to Bear Creek Mountain Stage

Two samples have ages that predate the Lake Creek stage. Sample GR16-07, collected from a basaltic lava flow northeast of Bear Creek Mountain, is from the Devils Washbasin volcano (Gusey et al., this volume). Groundmass from this sample yielded a  $^{40}$ Ar/ $^{39}$ Ar plateau age of  $2.68 \pm 0.01$  Ma (Fig. 3A), which we interpret as the eruption age for this lava flow. No absolute ages have been determined for the lava flows (or shallow intrusions) of Tieton Peak, but these rocks are normally magnetized like the Devils Washbasin basalts (Clayton, 1983; Swanson, 2017, written commun.). Based on the magnetization, the possible intercalation of the Tieton Peak and Devils Washbasin lavas (Clayton, 1983), and the basalt groundmass age, we tentatively assign the duration of Tieton Peak stage to within the normal subchron between 3.04 and 2.58 Ma at the end of the Gauss chron (Fig. 5; Cande and Kent, 1995).

Sample GR16-12, collected near Lost Lake, is the oldest andesite dated in this study. We take the eruption age to be  $2.27 \pm 0.01$  Ma based on the groundmass plateau age (Fig. 3B), which is within error of the groundmass total fusion age (2.25 ± 0.01 Ma; Supplementary Information DR1 [see footnote 1]) and the plagioclase plateau age of  $2.29 \pm 0.01$  Ma (Fig. 3C). Both the groundmass and plagioclase separates have age spectra that are discordant: The groundmass indicates slight <sup>39</sup>Ar recoil, and the plagioclase has a climbing age spectrum indicating slight excess argon. Although the groundmass plateau age has a higher MSWD than the 95% confidence limit for a homogeneous population (Mahon, 1996), we prefer it to the total fusion age, which includes anomalously young steps at high temperature (Fig. 3B). This lava flow was measured to have reversed magnetic polarity and was originally mapped as unit Qgr, from Lake Creek volcano, given its proximity to that eruptive center (Swanson, 1996b), but it is older than the Qgr, and Qgr, lavas that we analyzed. We arbitrarily include the andesite near Lost Lake with the Bear Creek Mountain stage on composition diagrams, but its eruptive stage remains undefined.

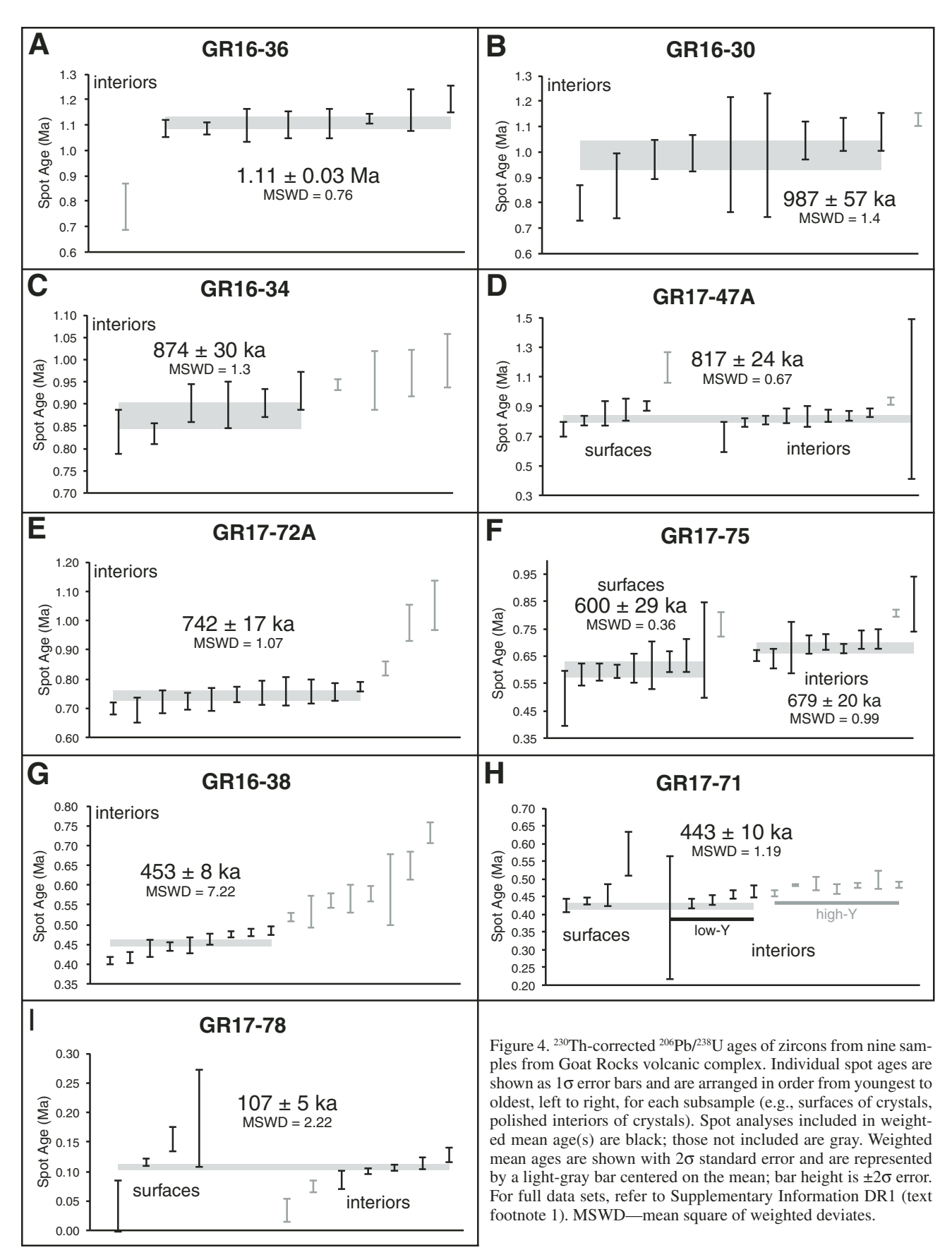
## Lake Creek Stage

Ages for each of the Lake Creek volcano map units (one sample from Qgr<sub>1</sub>, four from Qgr<sub>2</sub>, and one from Qgr<sub>3</sub>) indicate that Lake Creek volcano was active from at least 1.1 to 0.6 Ma. In addition, the dacite of Black Thumb erupted at ca. 0.8 Ma, and therefore we include it with the Lake Creek stage. Three of these samples yielded ages that appear to record brief magnetic excursions during the late Matuyama and Brunhes chrons. We retain the map units as assigned by Swanson, and further supported by our field magnetometer measurements, and rely on the <sup>40</sup>Ar/<sup>39</sup>Ar and U/Pb ages for age constraints.

The lowest lava flow in the Lake Creek sequence southeast of Goat Lake (sample GR16-36) marks the base of the normally magnetized unit Qgr, (Fig. 2; Swanson, 1996b). We take the eruption age to be  $1.11 \pm 0.01$  Ma, based on the groundmass total fusion age (Fig. 3D; Table 1). This age corresponds to the Punaruu normal magnetic excursion during the late Matuyama chron (1.12 Ma; Channell et al., 2002). Plagioclase from the same sample yielded a plateau age of  $1.13 \pm 0.01$  Ma and contains slight excess argon. Nevertheless, the plagioclase plateau age is within error of the groundmass total fusion age (Fig. 3E). Our U/Pb age for this sample is based on 12 spots analyzed on polished interiors of zircons (Fig. 4A). The youngest spot analysis was excluded from the weighted mean because it had high common Pb (29%) and did not overlap with others at  $1\sigma$  error. The youngest population of eight spots overlapping at  $1\sigma$  error yielded a weighted mean age (weighting by  $1\sigma$  spot error) of  $1.11 \pm 0.03$  Ma, which is within error of the 40Ar/39Ar groundmass total fusion age.

Zircon from sample GR16-30, collected from a dacite lava flow near the base of magnetically reversed unit  $Qgr_2$  (Fig. 2), yielded a U/Pb age of 987  $\pm$  57 ka from 10 spots analyzed on polished interiors (Fig. 4B). The oldest spot age overlapped at  $1\sigma$  error with younger spot ages, but we excluded it from the weighted mean because it is an outlier in composition (Th, U, and Y concentrations are more than double those of the main population; Table DR1 [see footnote 1]). The zircon crystallization age of this sample, considered to be a maximum estimate for eruption age, is within the magnetically reversed period from 988 to 925 ka (Horng et al., 2002).

The andesite lava flow capping Hawkeye Point (sample GR16-34) is at midsection in the reversely magnetized unit  $Qgr_2$ . Our <sup>40</sup>Ar/<sup>39</sup>Ar age determination for a groundmass separate yielded a plateau age of  $820 \pm 3$  ka (Fig. 3F), which we consider the eruption age for this lava flow. Spot analyses from polished zircons yielded a weighted mean age of  $920 \pm 33$  ka (MSWD = 2.5) including all 10 grains analyzed. This MSWD is larger than expected for a homogeneous population (e.g., Mahon, 1996), and so we prefer a weighted mean of the youngest six spots,  $874 \pm 30$  ka (MSWD = 1.3) as the zircon crystallization age (Fig. 4C). Each of these ages is within the magnetically reversed



period from 920 to 781 ka (Horng et al., 2002). We prefer the younger and more precise groundmass plateau age as the best estimate for the eruption age. The difference between the zircon age(s) and groundmass age suggests a protracted period of zircon crystallization prior to eruption, possibly in magma reservoirs that fed previous eruptions from Lake Creek volcano.

The U/Pb age of  $817 \pm 24$  ka for Black Thumb dacite (sample GR16-47A; Fig. 4D) indicates that this vent was active at the same time as Lake Creek volcano. This age is a weighted mean of spot analyses on both polished interiors and surfaces of zircons. Polished interiors alone yielded an age of  $822 \pm 27$  ka (MSWD = 0.60), excluding one resorbed-looking core that was slightly older than the weighted mean age at the  $1\sigma$  level. Seven spots on surfaces yielded an age of  $837 \pm 40$  ka (MSWD = 2.2), excluding two outliers that were also interpreted to be inherited crystals (Fig. 4D). Since the mean surface age and mean interior age overlapped at  $2\sigma$  error, we calculated a weighted mean of all spots included in those ages,  $817 \pm 24$  ka (MSWD = 0.67; Fig. 4D). Importantly, this age confirms that Black Thumb was not the source of the >1.3 Ma Tieton andesite flows (Table 1;

Fig. 5), as Gusey et al. (this volume) determined by comparing their bulk compositions.

An andesite lava flow (sample GR17-72A) within the upper normally magnetized unit  $Qgr_3$  from Lake Creek volcano yielded a U/Pb age of 742  $\pm$  17 ka from polished interiors of zircons. The age is a weighted mean of 11 spot ages overlapping at the  $1\sigma$  level; three older crystals were excluded (Fig. 4E). The age matches the normal magnetic polarity for this map unit as determined by Swanson (1996b) and this study (Fig. 5).

In accord with Swanson's (1996b) mapping of unit  $Qgr_2$ , we measured reversed magnetic polarity for the dacitic dike from which sample GR17-75 was collected (this sample is equivalent to GR15-02; Table 2). Surfaces of nine (out of 10) zircon crystals analyzed yielded a weighted mean age of  $600 \pm 29$  ka, which we take as the best estimate for the emplacement age for this dike (Fig. 4F). The one older surface spot age was interpreted as antecrystic and was excluded from this mean. The mean surface age is within error of two brief magnetic excursions during the early Brunhes chron: Big Lost (or stage 15a), recorded at 560–580 ka (575 ka), and stage 15b, at 605 ka (Laj and Channell, 2007; Lund

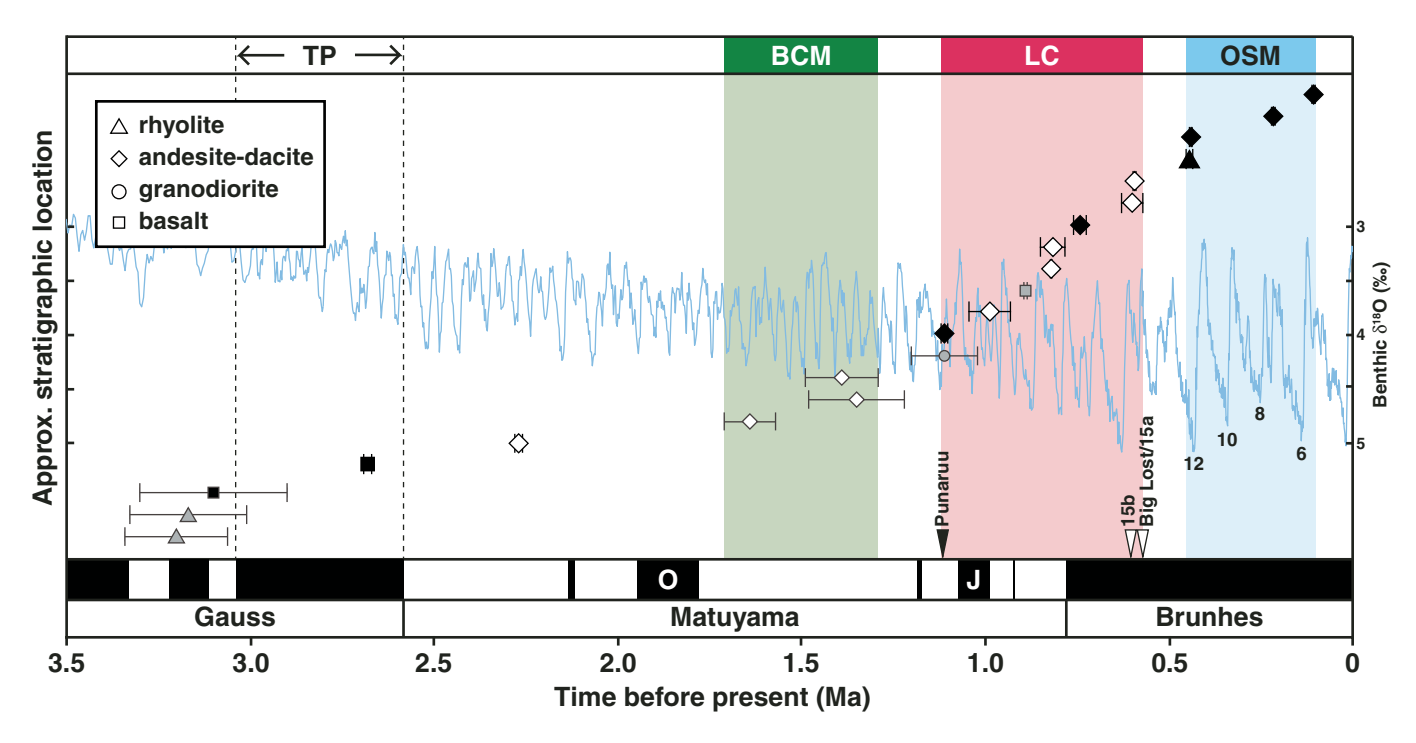


Figure 5. Eruptive timeline of the Goat Rocks volcanic complex, based on eruption ages from this study (large symbols) and ages from other studies (small symbols). Two erroneously old K/Ar ages for Devils Washbasin basalt and Hogback Mountain basalt by Clayton (1983) are excluded. Ages are arranged in stratigraphic order where stratigraphic relations are known and, otherwise, from oldest (bottom) to youngest (top). Error bars for each symbol show  $2\sigma$  error. Symbol color indicates magnetic polarity: normal (black), reversed (white), or undefined (gray). Note that for tuff along Miriam Creek and tuff below Tieton andesite (the sources of which are uncertain), the symbol used is for the overlying lava flow. Magnetic polarity time scale is compiled from Horng et al. (2002; <2.13 Ma) and Cande and Kent (1995; >2.13 Ma). O and J—Olduvai and Jaramillo subchrons, respectively. Labeled triangles indicate ages of brief magnetic excursions as reported by Channell et al. (2002), Lund et al. (2006), and Laj and Channell (2007). Colored columns show duration of major eruptive stages (BCM—Bear Creek Mountain, LC—Lake Creek, OSM—Old Snowy Mountain). The tentative duration of Tieton Peak stage (TP) is shown with dotted lines and is based on normal magnetic polarity and possible coevolution with Devils Washbasin basalt. Ages are overlain on the benthic  $\delta^{18}$ O record determined by Lisiecki and Raymo (2005). Select glacial marine isotope stages (MIS) are numbered; MIS 6 possibly corresponds to Hayden Creek Drift.

et al., 2006). Ten polished crystal interiors yielded nine spot ages overlapping at the  $1\sigma$  level and one outlier (Fig. 4F). The weighted mean of these nine spot ages is  $679 \pm 20$  ka, which is significantly older than the surface age, suggesting residence of crystallizing zircons of several tens of thousands of years.

Sample GR15-04 is from a magnetically reversed dacitic lava flow also from map unit Qgr<sub>2</sub>. Groundmass from this sample yielded a plateau age of  $593 \pm 4$  ka (Fig. 3G), which we take as the best estimate of the eruption age of this lava flow. This age is between, but close to, the reported ages for the Big Lost and stage 15b excursions (see previous paragraph). An amphibole separate yielded a plateau age of  $626 \pm 77$  ka (Fig. 3H), within error of the groundmass age.

## Old Snowy Mountain Stage

We determined ages for two samples from Old Snowy Mountain, one sample from Goat Ridge, and one sample of the Clear Fork andesite. Lavas from Old Snowy Mountain erupted from ca. 440 ka to <217 ka, broadly coeval with those at Goat Ridge, where a rhyolite low in the section yielded an age of ca. 443 ka. Clear Fork andesite, at ca. 107 ka, is the youngest lava flow yet dated in the Goat Rocks volcanic complex.

Sample GR16-38 of the Old Snowy Mountain andesite is low in the Old Snowy Mountain eruptive sequence, overlying Tertiary volcanic rock on the saddle east of Goat Lake (map number 67, Fig. 2). The eruption age is based on a groundmass separate that yielded a plateau age of  $440 \pm 3$  ka, based on highertemperature heating steps, despite slight <sup>39</sup>Ar recoil (Fig. 3I). Polished interiors of 17 zircon crystals yielded a complex range of ages. The weighted mean age of the youngest nine crystals is 453  $\pm$  8 ka (Fig. 4G). While the MSWD for this age (7.22) is much higher than expected for a homogeneous population (Mahon, 1996), it is challenging to isolate a smaller coherent population via composition or crystal appearance, given the relatively small number of grains analyzed. We therefore consider the zircon age to represent a complex and extended period(s) of pre-eruptive crystallization, and we prefer the groundmass 40Ar/39Ar plateau age as a better estimate for the eruption age.

For a dacitic lava flow higher in the Old Snowy Mountain section (sample GR16-25), the groundmass yielded a  $^{40}$ Ar/ $^{39}$ Ar plateau age of 217 ± 5 ka, which we assign as the eruption age for this lava flow (Fig. 3J).

Sample GR17-71 is from a rhyolite lava flow exposed in a creek drainage ~2 km west of the southern extent of Goat Ridge (map number 86, Fig. 2). This sample yielded a U/Pb age of  $443 \pm 10$  ka, which overlaps with early activity at Old Snowy Mountain (Figs. 4H and 5). Spot analyses on polished interiors of zircons from this sample define two compositional populations (a low-Y population with [Y] 359–1817 ppm, and a high-Y population with [Y] 2424–5655 ppm; Table DR1 [see footnote 1]), plus one older outlier (Fig. 4H). The weighted mean age of the younger, low-Y population (n = 5) is  $446 \pm 13$  ka (MSWD = 0.94). Four crystal surfaces group with the low-Y interior spots. The weighted mean of the surface spot ages is

 $438 \pm 16$  ka (MSWD = 1.7). Since the low-Y interior mean age and surface mean age overlap at  $2\sigma$  standard error, we prefer a combined mean age using all of the spots included in those two ages,  $443 \pm 10$  ka.

At  $107 \pm 5$  ka, the Clear Fork andesite (sample GR17-78; unit Qacf, Fig. 2) is the youngest at Goat Rocks to be dated thus far, while also bearing the longest record of zircon crystallization. The U/Pb age we determined is a weighted mean of spots from both interiors and surfaces of zircons. The youngest spot ages approach the limit of the resolution of U/Pb geochronology, so more scatter can be expected due to poor counting statistics on <sup>206</sup>Pb. Crystal interiors yielded a wide range of ages from 30 ka to 177 Ma, indicating many xenocrystic populations (see Table DR1 for full data set). Five of the seven analyses from zircon interiors gave a weighted mean age of  $104 \pm 6$  ka (MSWD = 1.8). We excluded the youngest two analyses in the population because they had high common Pb and were likely inaccurate. The youngest four of six surface analyses all contained high common Pb and were overall less precise, but they yielded a weighted mean age of 118 ± 13 ka (MSWD = 2.4), which overlaps with the age from interiors. We therefore prefer a weighted mean age of  $107 \pm 5$  ka including spot analyses from both surfaces and interiors (Fig. 4I). This age is younger than marine oxygen isotope stage (MIS) stage 6 (Fig. 5; Lisiecki and Raymo, 2005), which may correlate with the Hayden Creek glaciation (Evarts, 2005), supporting Swanson's (1996b) interpretation that the Clear Fork andesite erupted after that glacial event.

# **Rock Compositions**

The suite of Pliocene to Pleistocene volcanic rocks at Goat Rocks is dominantly andesites and dacites, with sparse rhyolites only in the early and late stages (Table 2; Fig. 6). A paucity of samples between 55 and 58 wt% SiO, separates the intermediate suite from contemporaneous basalts and basaltic andesites. These mafic samples fall within the field of mafic volcanic rocks in the southern Washington Cascades, but they do not extend to highly alkaline compositions (Fig. 7A). As a whole, the Goat Rocks andesite to rhyolite suite ranges from medium-K to high-K character, overlapping and spanning beyond the entire range of composition at neighboring arc volcanoes (Figs. 7A and 8). Two temporal patterns emerge. First, there is a general decrease in potassium (K) with time, with highest K<sub>2</sub>O in the Tieton Peak and Bear Creek Mountain stages, comparable to the high-K suite of Mount Adams, and lowest K<sub>2</sub>O in the Old Snowy Mountain suite, overlapping with the suite of Mount St. Helens (Figs. 7A and 8). We note that high-K compositions manifest at greater than ~59 wt% SiO<sub>2</sub>. The temporal potassium pattern at Goat Rocks mimics the spatial, trench-ward decrease in potassium in the arc, along with parallel declining Y, Zr, and Rb values, and increasing Sr/Y values (Fig. 9). The second temporal pattern is compositional restriction in the middle two stages compared to early and late stages, mainly owing to the absence of rhyolite. While we believe regional sampling has captured the variability of volcanic rocks, the number sampled is not a reliable proxy for relative volumes of the different stages.

The Tieton Peak stage has a wide range in bulk composition, but andesites dominate (Figs. 6 and 8).  $K_2O$ , Zr, and Y values reach their highest values during this stage, in comparison to later stages (Figs. 7A, 9C, and 9D), and concentrations of CaO, MgO, and particularly  $TiO_2$  are generally lower at a given weight percent  $SiO_2$ .

During the Bear Creek Mountain stage, the range in composition is restricted to mainly silicic andesite (Figs. 6 and 8C). Andesites of the Bear Creek Mountain stage have the highest K<sub>2</sub>O of the Goat Rocks suite, and for other elements, values define an upper or lower limit to the range of andesites (e.g., lowest Al<sub>2</sub>O<sub>3</sub>, FeO\*/MgO; highest TiO<sub>2</sub>, MgO, Rb, Zr; Figs. 7, 8, and 9).

The Lake Creek stage is the most voluminous, and most compositions are between 60 and 68 wt% SiO<sub>2</sub>, with scarce basaltic andesite (Figs. 6 and 8). This stage has the greatest range in incompatible elements (e.g., Zr, Rb, U, and Y; Fig. 9) among andesites and dacites and makes a compositional bridge between

potassic compositions of Bear Creek Mountain andesites and late, low-K compositions of the Old Snowy Mountain stage.

The Old Snowy Mountain stage is broad in composition  $(57-75 \text{ wt\% SiO}_2; \text{Fig. 6})$  and has two compositional modes, one at ~60–61 wt%  $\text{SiO}_2$  and one at ~67 wt%  $\text{SiO}_2$  (Fig. 8A). Andesites and dacites of Old Snowy Mountain stage differ from their predecessors not only in lower  $\text{K}_2\text{O}$ , Zr, and Y, but also in higher concentrations of  $\text{Al}_2\text{O}_3$  and Sr, resulting in high Sr/Y, one of the adakitic signatures defined by Defant and Drummond (1993); see Figures 7, 8, and 9.

#### **DISCUSSION**

The Goat Rocks volcanic complex provides new perspective into the timing of volcanism within the central Cascade arc. Here, we discuss how our new <sup>40</sup>Ar/<sup>39</sup>Ar and U/Pb ages refine both the eruptive timeline at Goat Rocks, as well as the magnetic polarity time scale recorded by its lavas. We then consider the size, longevity, and compositional variations at Goat Rocks and compare these to neighboring Cascade volcanoes.

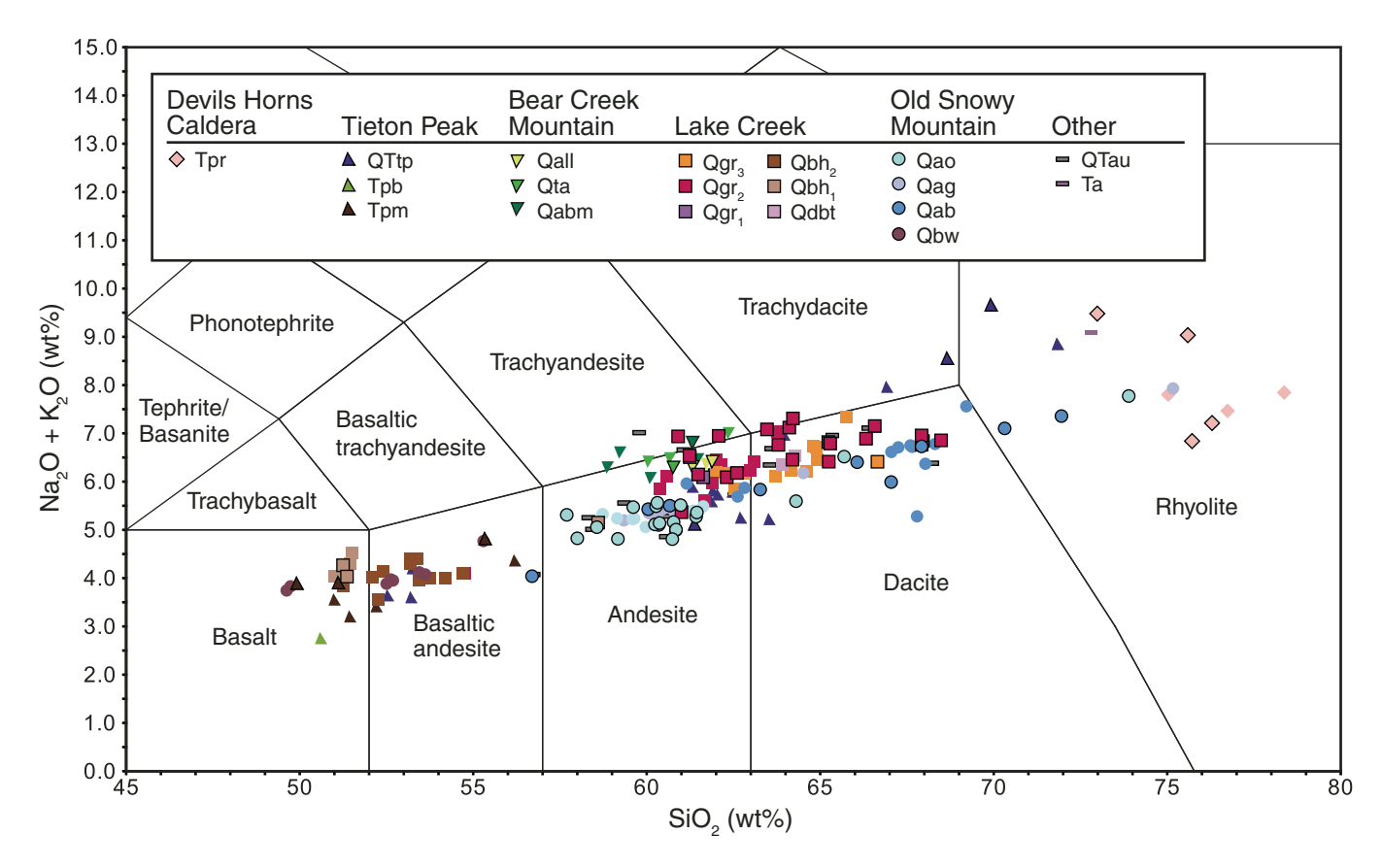


Figure 6. Total alkali-silica diagram for volcanic and shallow intrusive rocks of the Goat Rocks volcanic complex. Compositional fields are after Le Bas et al. (1986). Compositions of Devils Horns caldera (pre–Goat Rocks; pink diamonds) are included for reference. Symbol colors follow map unit colors in Figure 2. Symbols with black outlines are data newly presented in this paper; symbols with no outline include data from Swanson (1996a, 1996b), Clayton (1983), and Gusey et al. (this volume). For all composition data used in this figure and in Figures 7, 8, and 9, refer to Table DR2 (text footnote 1).

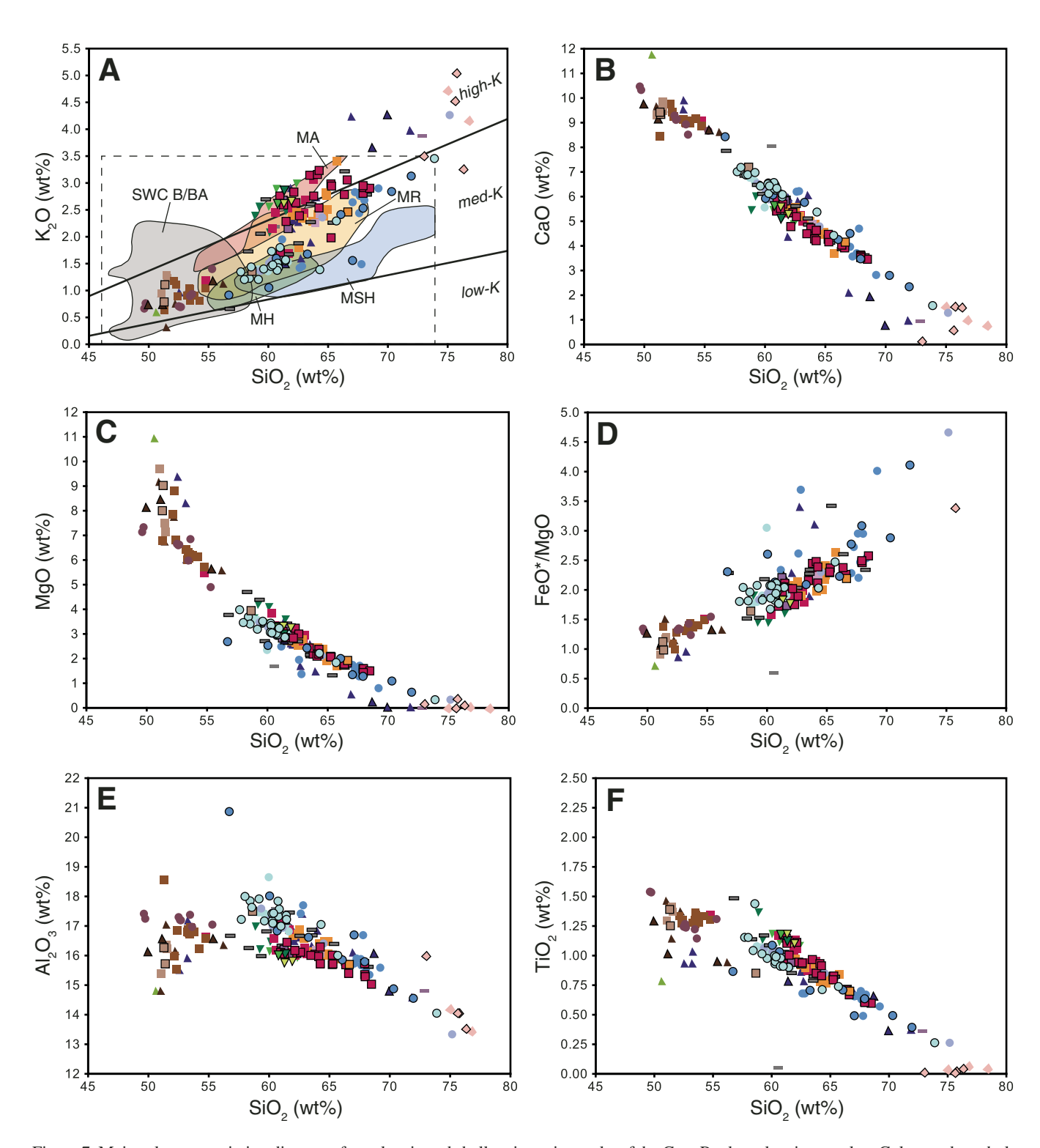
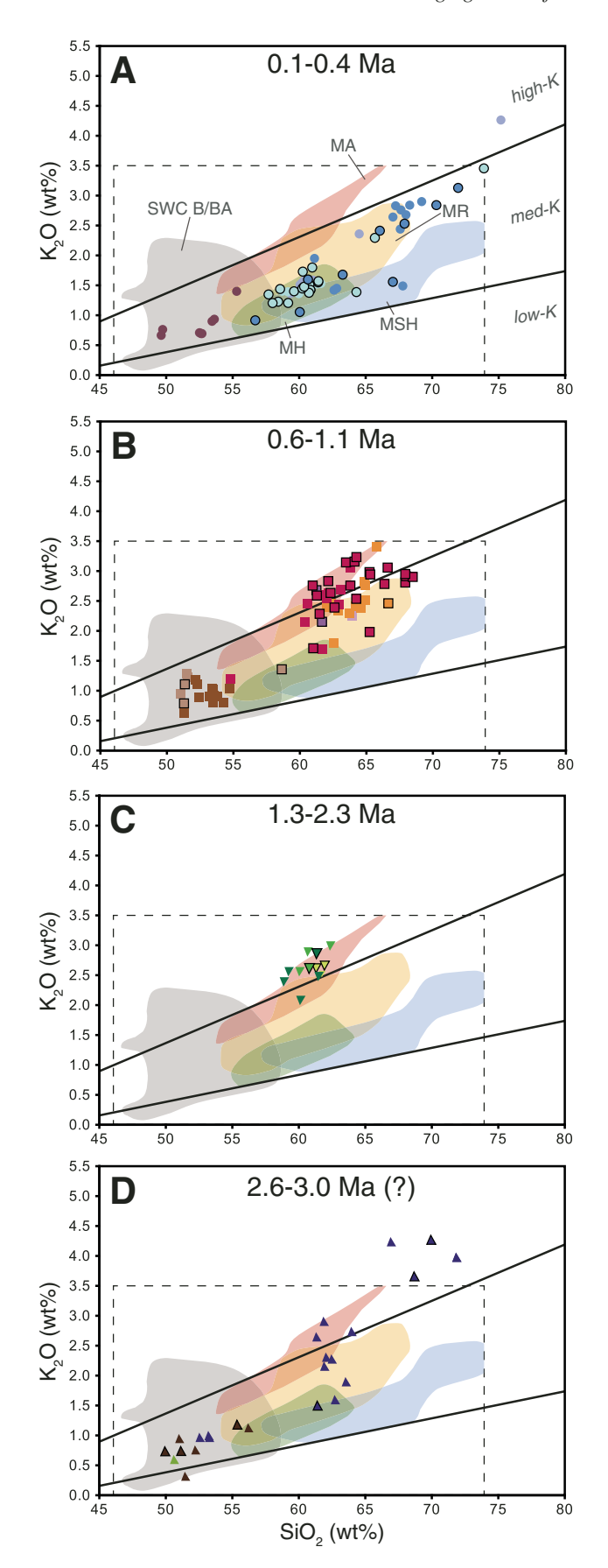


Figure 7. Major-element variation diagrams for volcanic and shallow intrusive rocks of the Goat Rocks volcanic complex. Colors and symbols are as in Figure 6. Dashed inset shows boundary of K<sub>2</sub>O diagram in Sisson et al. (2014). Fields for Mount Rainier (MR), Mount Adams (MA), Mount St. Helens (MSH), and Southern Washington Cascades basalt/basaltic andesite (SWC B/BA) are from data compiled by Sisson et al. (2014). K<sub>2</sub>O-SiO<sub>2</sub> field for Mount Hood (MH) was drafted from data presented in Scott et al. (1997).



# Integrating Magnetostratigraphy and Geochronology

Prior to this study, the chronology of the Goat Rocks volcanic complex was primarily based on magnetostratigraphy and calibrated with a handful of K-Ar, <sup>40</sup>Ar/<sup>39</sup>Ar, and zircon fission-track ages. While the overall chronology of eruptive stages has largely held true, our new ages refine these stages and reveal additional complexity in the Lake Creek volcanic sequence.

New ages indicate that the Lake Creek eruptive sequence captures multiple magnetic polarity subchrons and excursions during the late Matuyama to early Brunhes chrons. For example, early Qgr, lava sample GR16-36 (normally magnetized) has a groundmass age of  $1.11 \pm 0.1$  Ma, within uncertainty of the Punaruu normal excursion reported by previous authors (1.105 Ma—Singer et al., 1999; 1.115 Ma—Channell et al., 2002;  $1.075 \pm 0.032$  Ma—Ownby et al., 2007;  $1.095 \pm 0.210$  Ma— Michalk et al., 2013). The interval of time between this early Qgr, lava and the early Qgr, lava (reversed, e.g., GR16-30,  $987 \pm 57$  ka) also includes the Jaramillo normal subchron (Fig. 5). It is possible that all of the normally magnetized Qgr, lava flows were erupted during the brief ~5000 yr Punaruu excursion, or that eruptions continued over tens of thousands of years into the Jaramillo subchron; further work is required to constrain the ages of younger Qgr, lavas. In addition, lavas from map unit Qgr, are from multiple reversed periods, and they show that magnetic polarity alone cannot resolve age relationships where exposures are discontinuous or there are cryptic unconformities. Two Qgr<sub>a</sub> samples date to late Matuyama chron (GR16-30 and GR16-34), while two (GR17-75,  $600 \pm 29$  ka, and GR15-04,  $593 \pm 4$  ka) were erupted during a brief excursion in the early Brunhes chron (variable ages of potentially multiple excursions reported by Lund et al., 2006; Laj and Channell, 2007; Singer et al., 2008; Michalk et al., 2013), making them younger than a Qgr<sub>3</sub> lava flow that we dated (Table 1; Fig. 5). Full reconstruction of the growth of Lake Creek volcano awaits further chronologic calibration of more detailed magnetostratigraphy.

## Volcano Size and Volume

Extensive erosion makes it difficult to estimate the dimensions of the Goat Rocks volcanic complex during its construction. Clayton (1983) inferred that >60 km<sup>3</sup> of dominantly pyroxene andesite lava flows were erupted from a central volcanic edifice. Hildreth (2007) estimated 40 km<sup>3</sup> for the eroded remnants of the Goat Rocks. We estimate a total erupted volume

Figure 8. K<sub>2</sub>O vs. SiO<sub>2</sub> for samples from each eruptive stage of the Goat Rocks volcanic complex: (A) Old Snowy Mountain stage, (B) Lake Creek stage, (C) Bear Creek Mountain stage (plus Lost Lake andesite, though source of that lava flow is unknown), and (D) Tieton Peak stage. Age range of samples is shown at the top of each panel. Colors and symbols are as in Figure 6. Dashed inset and colored fields are as in Figure 7.

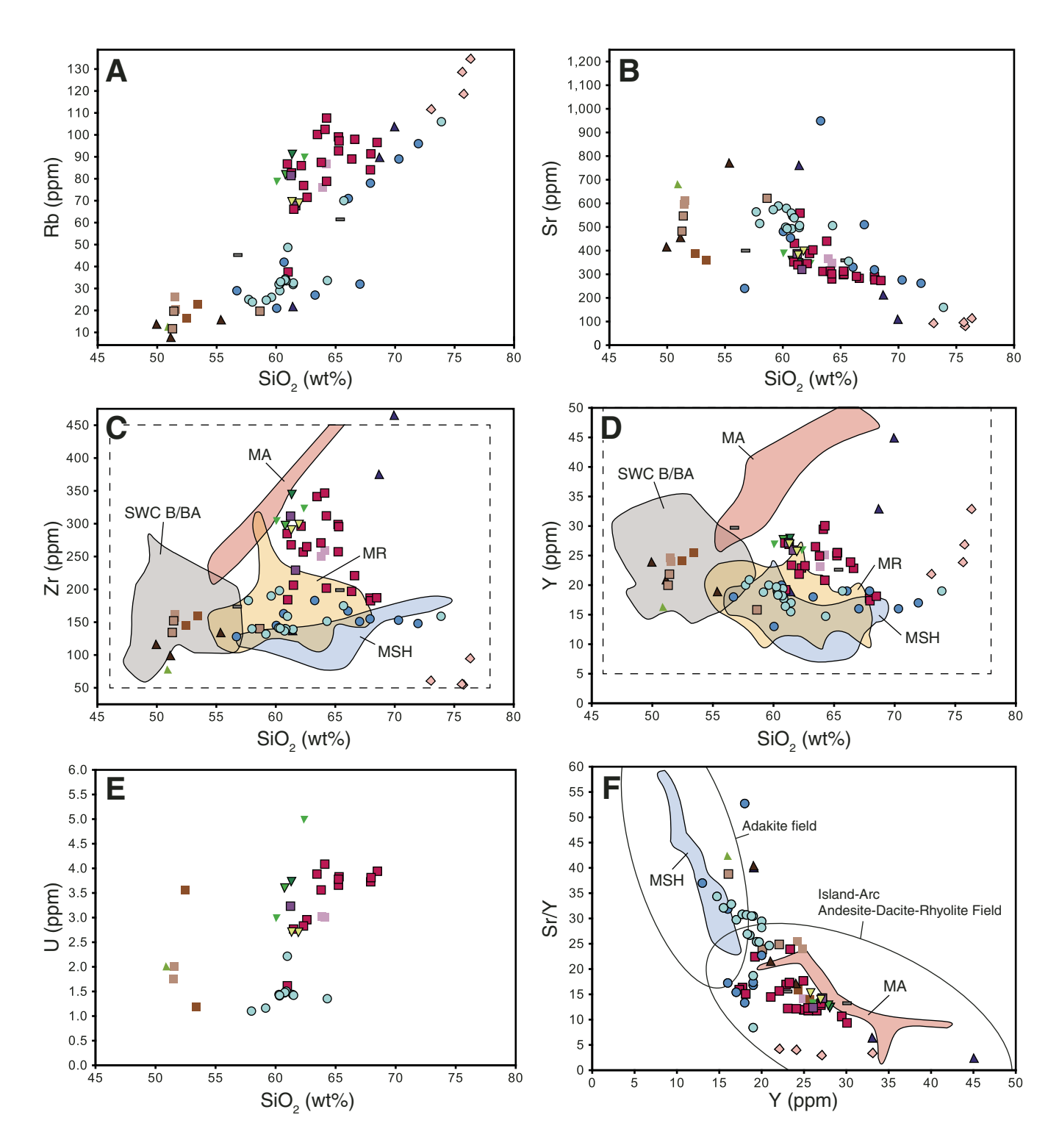


Figure 9. Trace-element variation diagrams for volcanic and shallow intrusive rocks of the Goat Rocks volcanic complex. Colors and symbols are as in Figure 6. All data shown are X-ray fluorescence (XRF) analyses, except for U (panel E), where inductively coupled plasmamass spectrometry (ICP-MS) data are shown for our new data (black outlines). Fields for Mount Rainier (MR), Mount Adams (MA), Mount St. Helens (MSH), and Southern Washington Cascades basalt/basaltic andesite (SWC B/BA) in panels C and D were drafted from data compiled by Sisson et al. (2014). Dashed insets in panels C and D show boundary of diagrams in Sisson et al. (2014). Fields for MSH and MA in panel F were drafted from data presented in Defant and Drummond (1993).

between 90 and 100 km<sup>3</sup> for the entire Goat Rocks volcanic complex, as follows.

The Lake Creek stage was the most voluminous and has a volcanic apron with a radius of at least 12 km from the inferred vent in the present-day valley of Upper Lake Creek. The radii of lava aprons around Mount Hood, Mount Adams, and Mount Rainier are slightly larger at ~14, 18, and 14 km, respectively, while the respective relief of their central peaks is 1800, 2300, and 2100 m above basement (Fig. 10; Hildreth, 2007). The ratio of relief to radius at these centers ranges from 0.13 to 0.15; applying these ratios to the lava radius at Goat Rocks (12 km) gives a range of 1500-1800 m relief. We make a conservative estimate of 1500 m for the full height of the Lake Creek volcano edifice above basement (Fig. 10). This relief is in keeping with the average relief of ~1565 m for 10 major Cascade andesitic volcanoes, excluding dome complexes and deeply glaciated or eroded centers (table 2 in Hildreth, 2007). Similarly, the average relief of Andean arc volcanoes in the Southern volcanic zone is ~1625 m,

independent of considerable variation in crustal thickness (Hildreth and Moorbath, 1988).

We estimated the volume of the Lake Creek volcano at ~60 km<sup>3</sup> by adding the volume of a central cone to that of a surrounding hollow disc. The inner 5-km-radius portion of the edifice can be approximated by a cone of height 1500 m and volume 40 km<sup>3</sup> (Fig. 10). The remaining volume of the lava apron is difficult to estimate: While preserved exposures of lava flows are as thick as 500 km in paleodrainages (Swanson, 1996b), this thickness is neither radially nor concentrically continuous. Estimating a distributed thickness of 50 m over the remaining hollow disc that extends to the 12 km radius, we calculate an additional ~20 km3 of lava and other ejecta for a total of ~60 km<sup>3</sup>. For comparison, the erupted volume of Mount Hood is estimated at 50–100 km<sup>3</sup> (Hildreth, 2007). If the other major andesitic vents (Tieton Peak, Bear Creek Mountain, Old Snowy Mountain) each contributed 10-15 km<sup>3</sup> (the Tieton andesite flows from Bear Creek Mountain add up to ~9 km<sup>3</sup>; Gusey et

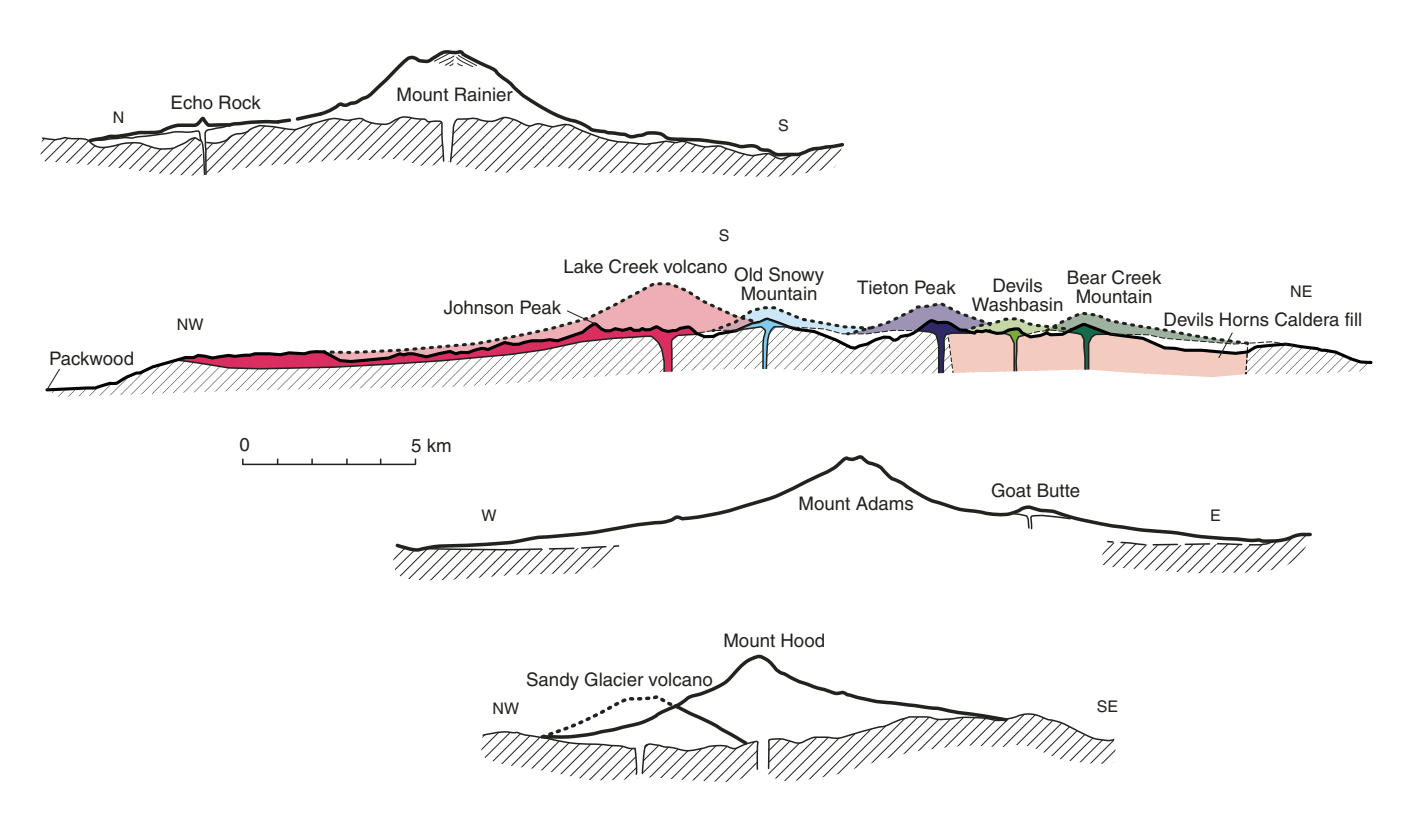


Figure 10. Schematic cross sections through major vents of the Goat Rocks volcanic complex. Note that cross section is bent ~90° near Old Snowy Mountain to capture existing deposits from each of the four main andesitic vents, so distance shown between nonadjacent vents may be greater than true distance (e.g., true distance between hypothesized Lake Creek volcano and Bear Creek Mountain summits is ~10 km). Bold solid line denotes present-day topography. Solid colors represent present-day thickness and extent of volcanic deposits interpreted from geologic maps, with conduits shown schematically. Diagonal stripes indicate basement rock. Original topography for each vent is projected schematically with dashed bold lines and pale colors. Note overlay between projected Old Snowy Mountain and Lake Creek volcanoes and between Bear Creek Mountain and Devils Washbasin, where younger eruptive products may have covered eroded surfaces where older deposits were once present (no crosscutting relations were observed in the field). The Devils Horns caldera ring fracture is fairly well constrained on the west side by a fault mapped north of Tieton Peak (Fig. 2; Swanson, 2017, written commun.), but its eastern extent is not well constrained, and the location shown here is for illustrative purpose only. Also included are profiles through nearby Mount Rainier, Mount Adams, and Mount Hood, after Hildreth (2007), all at the same scale with no vertical exaggeration.

al., this volume), the Goat Rocks volcanic complex as a whole could exceed 90 km<sup>3</sup> erupted volume.

#### Persistence of Andesite in the Cascade Arc

The life span of andesitic volcanism at Goat Rocks is 2.5–2.9 m.y., based on the magnetic correlation and possible intercalation of the oldest Tieton Peak stage andesite lavas with 2.7 Ma Devils Washbasin basalt. Eruptions of the subsequent Bear Creek Mountain stage occurred a few kilometers to the east and lasted at least 300,000 yr, from >1.6–1.3 Ma. The Lake Creek stage lasted ~500,000 yr, from 1.1 Ma to ca. 600 ka, during which time the Lake Creek volcano was constructed from an inferred center near Upper Lake Creek. This stage marks an ~10 km westward shift of the andesite focus. The youngest stage, Old Snowy Mountain stage, lasted ~330,000 yr from ca. 440 ka to 107 ka from regionally distributed vents.

Similarly persistent andesitic volcanism as at Goat Rocks occurred in the Mount Hood area. There, andesitic volcanism is as old as  $3.1 \pm 0.2$  Ma at Lookout Mountain, which is ~14 km to the east of Mount Hood (Wise, 1969; Sherrod and Scott, 1995). The Vista Ridge cone and Sandy Glacier volcano were active between 1.5 and 0.8 Ma and lie under and slightly west of Mount Hood, respectively. The modern edifice has been active since ca. 500 ka (Scott et al., 1997; Scott and Gardner, 2017).

Andesitic volcanism near Mount Rainier has persisted for at least ~1.4 m.y. Possibly juvenile clasts in the Lily Creek formation have been dated at  $1.36 \pm 0.05$  Ma and  $1.16 \pm 0.05$  Ma ( $2\sigma$  uncertainty; plagioclase  $^{40}$ Ar/ $^{39}$ Ar ages), and exposures at Panhandle Gap and Glacier Basin have been dated at  $1.06 \pm 0.05$  Ma

and  $1.03 \pm 0.00$  Ma (groundmass  $^{40}$ Ar/ $^{39}$ Ar ages), indicating that a previous edifice was active between ca. 1.4 and 1.0 Ma (Sisson and Calvert, 2017, written commun.). It is unknown whether activity continued between 1.0 Ma and the growth of the modern Rainier edifice, where activity had commenced by 0.6 Ma, based on two widely separated lavas dated at  $601 \pm 16$  ka and  $596 \pm 4$  ka (groundmass  $^{40}$ Ar/ $^{39}$ Ar ages; Sisson and Calvert, 2017, written commun.). Frequent voluminous eruptions, with major pulses from 500 to 420 ka and from 280 to 180 ka, built the present-day edifice (Sisson et al., 2001).

In the vicinity of Mount Adams, basaltic eruptions have occurred in a broad volcanic field since ca. 940 ka (Hildreth and Lanphere, 1994; Hildreth and Fierstein, 1995, 1997). The andesitic Hellroaring volcano was active from ca. 520 ka to 450 ka, when the eruptive center shifted ~5 km northwest to the modern Mount Adams vent (Hildreth and Lanphere, 1994; Hildreth and Fierstein, 1995, 1997). Like Mount Rainier, the Hellroaring volcano–Mount Adams edifice was built fitfully in major conebuilding episodes centered at ca. 500 ka, ca. 450 ka, and 30 ka, separated by lesser activity (Hildreth and Lanphere, 1994).

To the southwest of Goat Rocks, Mount St. Helens grew in stages a few tens to 100 k.y. long, resulting in a total volcanic history of ~300 k.y., but ages of entrained zircons suggest that intermediate magmatism was active for as long as 500–600 k.y. (Clynne et al., 2008; Claiborne et al., 2010). The modern stratocone was built only in the last 2.5 k.y. (Mullineaux and Crandell, 1981).

The record of andesite activity at Goat Rocks is comparable to Mount Hood and longer than at other neighboring centers (Fig. 11). The Lake Creek and Old Snowy Mountain stages

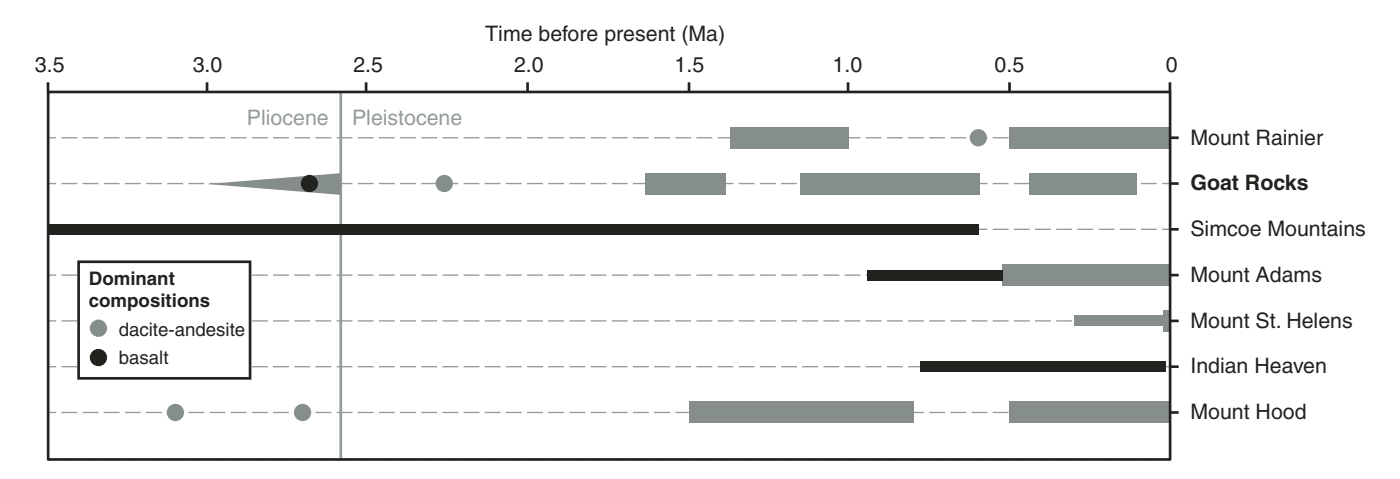


Figure 11. Eruptive history of Goat Rocks volcanic complex in context with regional volcanic activity. Eruptive history of an extinct volcano is included with an active volcano if it is located within ~15 km (approximate diameter of the Goat Rocks volcanic complex) of the modern edifice. Circles represent single eruptive events or separate deposits with statistically equivalent ages. Bars show extended periods of eruptive activity. Thick bars represent focused activity at a major edifice, while narrow bars show activity across a distributed area. Tapered bar on Goat Rocks timeline represents Tieton Peak stage, for which eruptive duration is tentatively constrained by Devils Washbasin basalt (black circle; see text) and magnetic polarity. Eruptive history sources are: Mount Rainier—Sisson et al. (2001) and Sisson and Calvert (2017, written commun.); Simcoe Mountains—Hildreth and Fierstein (2015); Mount Adams—Hildreth and Lanphere (1994); Mount St. Helens—Mullineaux and Crandell (1981) and Clynne et al. (2008); Indian Heaven—Mitchell et al. (1989) and Korosec (1989); and Mount Hood—Sherrod and Scott (1995) and Scott et al. (1997).

together represent a nearly continuous period of eruptive activity lasting 1 m.y., comparable to the 0.7 m.y. period of activity at Vista Ridge and Sandy Glacier volcanoes (Mount Hood predecessors). If the long life span of the Goat Rocks volcanic complex is an analog, then one might expect Mount Hood to be near the end of its life, and other neighboring centers can expect another 0.5–1.5 m.y. of activity.

A picture emerges in which at ca. 2.5 Ma, Tieton Peak and Lookout Mountain (Mount Hood area) dominated the arc at these latitudes. At ca. 1.5 Ma, proto—Mount Rainier, Bear Creek Mountain, and Vista Ridge and/or Sandy Glacier volcanoes were active. Flare-ups at Mount Rainier and Mount Adams at ca. 500 ka coincided with the onset of the modern cone at Mount Hood and with the end of the productive Lake Creek volcano. Less-voluminous, more-distributed activity at Goat Rocks followed Lake Creek volcano during the Old Snowy Mountain stage. Mount St. Helens emerged during this final Goat Rocks stage and became increasingly productive as activity at Goat Rocks ended. In summary, the Goat Rocks volcanic complex further illuminates an arc-wide history of waxing and waning of andesitic arc volcanoes, which invites speculation about the distribution of energy delivered from the mantle to the crust at subduction zones.

# **Geochemical Variations through Time**

The Goat Rocks volcanic complex has a wide range of compositions and is an excellent case for grappling with the complex processes that produce andesitic arc volcanoes. Abundant quenched inclusions of variably more mafic magmas, large ranges in composition at similar silica contents, and diverse populations of zircons attest to a complex magmatic history typical of arc volcanoes. While a comprehensive petrologic treatment awaits fuller characterization of the suite, we point out some major patterns and their implications. We first address variability within the Goat Rocks suite, and then we consider the temporal pattern of larger compositional variability in the early and late stages compared to the middle two stages. Finally, we compare the temporal pattern toward less-potassic, adakite-like compositions to across-arc variations.

# Stages of the Goat Rocks Volcanic Complex

The Tieton Peak stage has high-K silicic compositions, moderate-K mafic compositions, and an array of varied-K intermediate compositions (Figs. 7 and 8). Lower Ti in the mafic compositions compared to the rest of the Goat Rocks suite suggests a different mantle contribution for this part of the suite (Fig. 9). The high variability of potassium among andesites, without a high-K mafic parent, implies that the high-K signature was crustally derived.

The Bear Creek Mountain stage produced tightly clustered andesites that are as potassic as the high-K andesites of Tieton Peak stage, but they differ from those in having higher Ti and lower Sr compositions (Figs. 7, 8, and 9), thus putting them on a different liquid line of descent more akin to highest-K andesites

of the Lake Creek stage. Andesites and dacites of the Bear Creek Mountain and Lake Creek stages are tightly clustered along similar major-element trends. Declining CaO, Al<sub>2</sub>O<sub>3</sub>, and Sr with increasing silica (Figs. 7B, 7E, and 9B) signal plagioclase-dominated fractionation. On the other hand, strong scatter with respect to incompatible elements, including K and Rb, indicates a complex of processes, likely variable proportions of crystal fractionation, magma mixing, and crustal assimilation, to be unraveled in future work. The Lake Creek stage also includes compositions with lower K<sub>2</sub>O, transitional to the Old Snowy Mountain stage. No rhyolites were erupted during these middle two stages.

The Old Snowy Mountain stage is distinct from the middle stages in having a wide compositional spread and the most linear distribution of data among the four stages on both majorand trace-element variation diagrams (Figs. 7 and 9). The linear trends suggest a dominance of magma mixing between mafic andesite and a rhyolitic composition similar to that of Devils Horns. Higher Al<sub>2</sub>O<sub>3</sub> among mafic andesites indicates suppression of plagioclase in their derivation, likely owing to deeper and (or) wetter conditions, consistent with more phenocrystic amphibole in this suite. While most of the data fall along a moderate K-enrichment with silica, overlapping the field of Mount Rainier, a smattering of samples define a separate trend similar to the relatively K-poor andesites and dacites of Mount St. Helens.

#### Compositional Range in Time

Volcanism at Goat Rocks is strongly dominated by silicic andesite and dacite, especially in the middle eruptive stages, but it varies from basaltic andesite to rhyolite in early and late stages (Fig. 7). The pattern invites comparison to other long-lived intermediate suites, where volcanism exhibits a middle period of restricted composition that also corresponds to the largest erupted volume (e.g., Aucanquilcha volcanic cluster and other examples—Grunder et al., 2006; Yanacocha volcanics—Longo et al., 2010; eastern Great Basin-Gans et al., 1989; Mount Jefferson volcanic field—Conrey et al., 2001; DiGiulio, 2016). We postulate that the more homogeneous phase represents a time when the magmatic underpinnings of the complex were well established, creating an extensive mushy zone in the crust where more mafic rising magmas were trapped and hybridized (e.g., Aucanquilcha volcanic cluster; Walker et al., 2012) and rhyolitic crustal melts were effectively assimilated. Basaltic magmas could have ascended and erupted before and after the creation of the mushy crustal magma complex, or they may have penetrated along the margins (the shadow zone effect; e.g., Walker, 2000).

# Adakitic Signature in Time versus Space

The Old Snowy Mountain stage has the highest Sr/Y of the Goat Rocks suite (Fig. 9F), an adakitic indicator defined by Defant and Drummond (1993). Such an adakitic signature can be acquired by melting of the slab, which is an appealing interpretation for the young hot slab beneath Cascadia. Although we cannot at this point exclude mantle-hosted influence, the temporal context for the adakitic signature in the last stage of a protracted

andesitic history suggests that the adakitic character was derived during crustal residence. Smith and Leeman (1987) argued that the adakitic character of the Mount St. Helens dacite reflects deep amphibolite-derived crustal magma sources. Contribution of deep, young mafic sources has been supported by Os isotopic studies at Mount Adams (Jicha et al., 2009). In an analysis of across-arc increases in  $K_2O$  in the central Andes, Michelfelder et al. (2013) proposed amphibolitic crustal influence for less potassic arc-front volcanoes and the influence of increasingly felsic crust with distance from the arc to produce more potassic suites. In any case, at Goat Rocks, the temporal compositional changes within a relatively confined area mimic the transarc variability in southern Washington, and they can serve as a test for the significance of these spatial variations.

#### CONCLUSION

The Goat Rocks volcanic complex is a long-lived Pliocene to Pleistocene andesitic locus in the southern Washington Cascades. Goat Rocks was active over a period of ~2.5–2.9 m.y., from at least 2.6 Ma (and possibly as long ago as 3.0 Ma) to ca. 100 ka. Activity at Goat Rocks occurred in four stages from vents within an ellipsoidal area of ~200 km², surrounded by contemporaneous mafic vents.

- (1) The Tieton Peak stage (tentatively 3.0–2.6 Ma) marks the onset of activity at Goat Rocks. Volcanism was centered at Tieton Peak, overlapping the margin of the 3.2 Ma Devils Horns rhyolite caldera. The compositional range is broad, ranging from basaltic andesite to rhyolite.
- (2) During the Bear Creek Mountain stage (>1.6–1.3 Ma), eruptions occurred at Bear Creek Mountain and included the Tieton andesite lavas that flowed as far as 74 km down paleovalleys to the east (Gusey et al., 2018, this volume). In contrast to the Tieton Peak stage, compositions are restricted to high-K andesites.
- (3) During the Lake Creek stage (1.1–0.6 Ma), an ~3500-m-high, ~60 km³, andesite-dacite composite cone was constructed at what is now the Upper Lake Creek basin. Andesite and dacite lavas extended to a radius of at least 12 km. This was the most voluminous, climactic stage at Goat Rocks, dominated by compositionally variable andesites and dacites.
- (4) The Old Snowy Mountain stage (0.4–0.1 Ma) included eruptions at Old Snowy Mountain and from distributed vents across the Goat Rocks area. This suite marks the waning of volcanism at Goat Rocks and includes diverse compositions from basaltic andesite to rhyolite.

Early in the Goat Rocks eruptive history, the main andesitic volcanoes in this region of the Cascade arc were Tieton Peak and proto–Mount Hood. At the time of Bear Creek Mountain to Lake Creek volcano, Mount Rainier and Mount Adams emerged. With the growth of Mount St. Helens, activity at Goat Rocks waned and ceased.

Volcanic rock compositions of the Goat Rocks suite are less potassic with time: Tieton Peak through Lake Creek stages generally constitute a high-K suite, while vents of the Old Snowy Mountain stage erupted medium-K compositions. Magmas of the Old Snowy Mountain stage were more water-rich, as indicated by higher Al<sub>2</sub>O<sub>3</sub> compositions and a prevalence of amphibole. The compositional changes through time at Goat Rocks mimic the compositional diversity across the Cascade arc: earlier magmas are more Mount Adams-like, while some Old Snowy Mountain stage magmas are similar to Mount St. Helens compositions. We attribute the change to a more adakitic character to the influences of more mafic crust and more water in differentiation.

#### **ACKNOWLEDGMENTS**

This work was supported by National Science Foundation Graduate Research Fellowship grant 1314109-DGE, and also by grants EAR-1358514, 1358554, 1358401, 1358443, and 1101100 (Earthscope National Office). Any opinions, findings, and conclusions or recommendations expressed in this material are those of the authors and do not necessarily reflect the views of the National Science Foundation. Thanks go to the Earthscope AGeS program for its support. A 2016 Geological Society of America graduate student research grant and a 2017 Jack Kleinman grant also supported this work. We deeply thank Don Swanson for providing his mapping and analytical data for inclusion in this project, and for discussion, guidance, and inspiration. We are grateful to reviewers Brian Jicha and Gary Michelfelder, whose insights improved this manuscript, and to Mike Garcia, for attentive editorial handling. Thanks go to the Washington State University GeoAnalytical Laboratory and Nansen Olson for support in sample preparation and data interpretation. We appreciate discussions and coordination with Daryl Gusey, including a tour of the Tieton andesite in summer 2016. We also appreciate discussions with Tom Sisson, Andy Calvert, Judy Fierstein, Wes Hildreth, and Daniel Heaton. William Otto, Nathan Van Cleave, Tommy Moore, Peter Davidson, Zoe Dilles, Marina Marcelli, and Nansen Olson provided essential support during fieldwork in 2016 and 2017.

# REFERENCES CITED

- Bacon, C.R., Bruggman, P.E., Christiansen, R.L., Clynne, M.A., Donnelly-Nolan, J.M., and Hildreth, W., 1997, Primitive magmas at five Cascade volcanic fields: Melts from hot, heterogeneous sub-arc mantle: Canadian Mineralogist, v. 35, p. 397–423.
- Barth, A.P., and Wooden, J.L., 2010, Coupled elemental and isotopic analyses of polygenetic zircons from granitic rocks by ion microprobe, with implications for melt evolution and the sources of granitic magmas: Chemical Geology, v. 277, no. 1–2, p. 149–159, https://doi.org/10.1016/j.chemgeo.2010.07.017.
- Black, L.P., Kamo, S.L., Allen, C.M., Davis, D.W., Aleinikoff, J.N., Valley, J.W., Mundil, R., Campbell, I.H., Korsch, R.J., Williams, I.S., and Foudoulis, C., 2004, Improved <sup>206</sup>Pb/<sup>238</sup>U microprobe geochronology by the monitoring of a trace-element-related matrix effect; SHRIMP, IDTIMS, ELA-ICP-MS and oxygen isotope documentation for a series of zircon standards: Chemical Geology, v. 205, p. 115–140, https://doi.org/10.1016/j.chemgeo.2004.01.003.
- Bowles-Martinez, E., Bedrosian, P., Schultz, A., Hill, G.J., and Peacock, J., 2016, The Southern Washington Cascades magmatic system imaged

- with magnetotellurics: San Francisco, California, American Geophysical Union, 2016 Fall Meeting, abstract GP41A–01.
- Cande, S.C., and Kent, D.V., 1995, Revised calibration of the geomagnetic polarity timescale for the Late Cretaceous and Cenozoic: Journal of Geophysical Research, v. 100, no. B4, p. 6093–6095, https://doi.org/ 10.1029/94JB03098.
- Channell, J.E.T., Mazaud, A., Sullivan, P., Turner, S., and Raymo, M.E., 2002, Geomagnetic excursions and paleointensities in the Matuyama chron at Ocean Drilling Program Sites 983 and 984 (Iceland Basin): Journal of Geophysical Research, v. 107, no. B6, p. EPM 1-1–EPM 1-14, https://doi.org/10.1029/2001JB000491.
- Claiborne, L.L., Miller, C.F., Flanagan, D.M., Clynne, M.A., and Wooden, J.L., 2010, Zircon reveals protracted magma storage and recycling beneath Mount St. Helens: Geology, v. 38, no. 11, p. 1011–1014, https://doi.org/ 10.1130/G31285.1.
- Clayton, G., 1980, Geology of the White Pass-Tumac Mountain Area, Washington: Washington Division of Geology and Earth Resources Open-File Report 80-8, scale 1:24,000.
- Clayton, G., 1983, Geology of the White Pass Area, South-Central Cascade Range, Washington [M.S. thesis]: Seattle, Washington, University of Washington, 212 p.
- Clynne, M.A., Calvert, A.T., Edward, W.W., Evarts, R.C., Fleck, R.J., and Lanphere, M.A., 2008, The Pleistocene eruptive history of Mount St. Helens, Washington, from 300,000 to 12,800 years before present, in Sherrod, D., Scott, W.E., and Stauffer, P.H., eds., A Volcano Rekindled: The Renewed Eruption of Mount St. Helens, 2004–2006: U.S. Geological Survey Professional Paper 1750, p. 593–627.
- Coble, M.A., Burgess, S.D., and Klemetti, E.W., 2017, New zircon (U-Th)/ He and U/Pb eruption age for the Rockland tephra, western USA: Quaternary Science Reviews, v. 172, p. 109–117, https://doi.org/10.1016/j.quascirev.2017.08.004.
- Colman, S.M., and Pierce, K.L., 1981, Weathering Rinds on Andesitic and Basaltic Stones as a Quaternary Age Indicator, Western United States: U.S. Geological Survey Professional Paper 1210, 56 p.
- Conrey, R.M., Sherrod, D.R., Hooper, P.R., and Swanson, D.A., 1997, Diverse primitive magmas in the Cascade arc, northern Oregon and southern Washington: Canadian Mineralogist, v. 35, p. 367–396.
- Conrey, R.M., Hooper, P.R., Larson, P.B., Chesley, J., and Ruiz, J., 2001, Traceelement and isotopic evidence for two kinds of crustal melting beneath a high Cascades volcanic center: Contributions to Mineralogy and Petrology, v. 141, p. 710–732, https://doi.org/10.1007/s004100100259.
- Conrey, R.M., Taylor, E.M., Donnelly-Nolan, J.M., and Sherrod, D.R., 2002, North-central Oregon Cascades: Exploring petrologic and tectonic intimacy in a propagating intra-arc rift, in Moore, G.W., ed., Field Guide to Geologic Processes in Cascadia: Oregon Department of Geology and Mineral Industries Special Paper 36, p. 47–90.
- Conrey, R.M., Grunder, A.L., and Schmidt, M.E., 2004, SOTA Field Trip Guide—State of the Cascade Arc: Stratocone Persistence, Mafic Lava Shields, and Pyroclastic Volcanism Associated with Intra-Arc Rift Propagation: Oregon Department of Geology and Mineral Industries Open-File Report O-04-04, 40 p.
- Crandell, D.R., 1987, Deposits of Pre-1980 Pyroclastic Flows and Lahars from Mount St. Helens, Washington: U.S. Geological Survey Professional Paper 1444, 91 p.
- Crowley, J.L., Schoene, B., and Bowring, S.A., 2007, U-Pb dating of zircon in the Bishop Tuff at the millennial scale: Geology, v. 35, no. 12, p. 1123–1126, https://doi.org/10.1130/G24017A.1.
- de Bremond d'Ars, Jaupart, C., and Sparks, R.S.J., 1995, Distribution of volcanoes in active margins: Journal of Geophysical Research, v. 100, p. 20,421–20,432, https://doi.org/10.1029/95JB02153.
- Defant, M.J., and Drummond, M.S., 1993, Mount St. Helens: Potential example of the partial melting of the subducted lithosphere in a volcanic arc: Geology, v. 21, p. 547–550, https://doi.org/10.1130/0091-7613 (1993)021<0547:MSHPEO>2.3.CO;2.
- Dethier, D.P., 1988, The Soil Chronosequence along the Cowlitz River, Washington: U.S. Geological Survey Bulletin 1590-F, p. F1–F47.
- DiGiulio, J., 2016, Reconstructing the Physical Record of a Four-Million-Year Volcanic System: Geochemistry, Thermobarometery and Geologic Map of the Mount Jefferson Area, Oregon [M.S. thesis]: Corvallis, Oregon, Oregon State University, 119 p.
- Ellingson, J.A., 1968, Late Cenozoic Volcanic Geology of the White Pass–Goat Rocks Area, Cascade Mountains, Washington [Ph.D. dissertation]: Pullman, Washington, Washington State University, 112 p.

- Evarts, R.C., 2005, Geologic Map of the Amboy Quadrangle, Clark and Cowlitz Counties, Washington: U.S. Geological Survey Scientific Investigations Map 2885, 1 sheet, 26 p. text.
- Evarts, R.C., Clynne, M.A., Fleck, R.J., Lanphere, M.A., Calvert, A.T., and Sarna-Wojcicki, A.M., 2003, The antiquity of Mount St. Helens and age of the Hayden Creek Drift: Geological Society of America Abstracts with Programs, v. 35, no. 6, p. 80.
- Gans, P.B., Mahood, G.A., and Schermer, E., 1989, Synextensional Magmatism in the Basin and Range Province; a Case Study from the Eastern Great Basin: Geological Society of America Special Paper 233, 53 p., https:// doi.org/10.1130/SPE233-p1.
- Gill, J.B., 1981, Orogenic Andesites and Plate Tectonics: Berlin, Springer Verlag, 390 p., https://doi.org/10.1007/978-3-642-68012-0.
- Grunder, A.L., Klemetti, E.W., Feeley, T.C., and McKee, C.M., 2006, Eleven million years of arc volcanism at the Aucanquilcha volcanic cluster, northern Chilean Andes: Implications for the life span and emplacement of plutons: Transactions of the Royal Society of Edinburgh–Earth Sciences, v. 97, p. 415–436, https://doi.org/10.1017/S0263593300001541.
- Guffanti, M., and Weaver, C.S., 1988, Distribution of late Cenozoic volcanic vents in the Cascade Range: Volcanic arc segmentation and regional tectonic considerations: Journal of Geophysical Research, v. 93, p. 6513– 6529, https://doi.org/10.1029/JB093iB06p06513.
- Gusey, D.L., Hammond, P.E., and Lasher, J.P., 2018, this volume, Tieton andesite, south-central Washington Cascades: Two of the longest known andesite lava flows, in Poland, M., Garcia, M., Camp, V., and Grunder, A., eds., Field Volcanology: A Tribute to the Distinguished Career of Don Swanson: Geological Society of America Special Paper 538, https://doi.org/10.1130/2018.2538(05).
- Hammond, P.E., 1980, Reconnaissance Geologic Map and Cross Sections of Southern Washington Cascade Range: Portland, Oregon, Portland State University, Publications of Department of Earth Science, scale 1:125,000.
- Hammond, P.E., 2017, Geologic Map of the Northern Portions of the Rimrock Lake, Tieton Basin, and Western Two-Thirds of the Weddle Canyon 7.5-Minute Quadrangles, Yakima County, Washington: Washington Geological Survey Map Series 2017-03, scale 1:24,000, 1 sheet, 19 p. text.
- Hildreth, W., 2007, Quaternary Magmatism in the Cascades: Geologic Perspectives: U.S. Geological Survey Professional Paper 1744, 125 p.
- Hildreth, W., and Fierstein, J., 1995, Geologic Map of the Mount Adams Volcanic Field, Cascade Range of Southern Washington: U.S. Geological Survey Map I-2460, scale 1:50,000, 2 sheets, 39 p. text.
- Hildreth, W., and Fierstein, J., 1997, Recent eruptions of Mount Adams, Washington Cascades, USA: Bulletin of Volcanology, v. 58, p. 472–490, https://doi.org/10.1007/s004450050156.
- Hildreth, W., and Fierstein, J., 2015, Geologic Map of the Simcoe Mountains Volcanic Field, Main Central Segment, Yakama Nation, Washington: U.S. Geological Survey Scientific Investigations Map 3315, scale 1:24,000, 3 sheets, 76 p. text.
- Hildreth, W., and Lanphere, M.A., 1994, Potassium-argon geochronology of a basalt-andesite-dacite arc system: The Mount Adams volcanic field, Cascade Range of southern Washington: Geological Society of America Bulletin, v. 106, p. 1413–1429, https://doi.org/10.1130/0016 -7606(1994)106<1413:PAGOAB>2.3.CO;2.
- Hildreth, W., and Moorbath, S., 1988, Crustal contributions to arc magmatism in the Andes of central Chile: Contributions to Mineralogy and Petrology, v. 98, p. 455–489, https://doi.org/10.1007/BF00372365.
- Hill, G.J., Caldwell, T.G., Heise, W., Chertkoff, D.G., Bibby, H.M., Burgess, M.K., Cull, J.P., and Cas, R.A.F., 2009, Distribution of melt beneath Mount St. Helens and Mount Adams inferred from magnetotelluric data: Nature Geoscience, v. 2, p. 785–789, https://doi.org/10.1038/ngeo661.
- Horng, C.-S., Lee, M.-Y., Pälike, H., Wei, K.-Y., Liang, W.-T., Iizuka, Y., and Torii, M., 2002, Astronomically calibrated ages for geomagnetic reversals within the Matuyama chron: Earth, Planets, and Space, v. 54, p. 679–690, https://doi.org/10.1186/BF03351719.
- Hughes, S.S., and Taylor, E.M., 1986, Geochemistry, petrogenesis, and tectonic implications of central High Cascade mafic platform lavas: Geological Society of America Bulletin, v. 97, p. 1024–1036, https://doi.org/10.1130/0016-7606(1986)97<1024:GPATIO>2.0.CO;2.
- Ireland, T.R., and Williams, I.S., 2003, Considerations in zircon geochronology by SIMS: Reviews in Mineralogy and Geochemistry, v. 53, p. 215–241, https://doi.org/10.2113/0530215.
- Jicha, B.R., and Singer, B.S., 2006, Volcanic history and magmatic evolution of Seguam Island, Aleutian Island arc, Alaska: Geological Society of

America Bulletin, v. 118, no. 7–8, p. 805–822, https://doi.org/10.1130/B25861.1.

- Jicha, B.R., Johnson, C.M., Hildreth, W., Beard, B.L., Hart, G.L., Shirey, S.B., and Singer, B.S., 2009, Discriminating assimilants and decoupling deep-vs. shallow-level crystal records at Mount Adams using <sup>238</sup>U–<sup>230</sup>Th disequilibria and Os isotopes: Earth and Planetary Science Letters, v. 277, no. 1–2, p. 38–49, https://doi.org/10.1016/j.epsl.2008.09.035.
- Johnson, D.M., Hooper, P.R., and Conrey, R.M., 1999, XRF analysis of rocks and minerals for major and trace elements on a single low dilution Litetraborate fused bead: Advances in X-ray Analysis, v. 41, p. 843–867.
- Kelly, D., 2016, Estimation of analytical error for major, minor and trace elements analyzed by X-ray fluorescence at the Peter Hooper GeoAnalytical Laboratory, Washington State University: Geological Society of America Abstracts with Programs, v. 48, no. 7, paper no. 324-12, https://doi.org/10.1130/abs/2016AM-284288.
- Koppers, A.A.P., 2002, ArArCALC—Software for <sup>40</sup>Ar/<sup>39</sup>Ar age calculations: Computers & Geosciences, v. 28, p. 605–619 (available at http://earthref.org/tools/ararcalc.htm), https://doi.org/10.1016/S0098-3004(01)00095-4.
- Koppers, A.A.P., Staudigel, H., Pringle, M.S., and Wijbrans, J.R., 2003, Short-lived and discontinuous intraplate volcanism in the South Pacific: Hot spots or extensional volcanism?: Geochemistry Geophysics Geosystems, v. 4, 1089, https://doi.org/10.1029/2003GC000533.
- Korosec, M.A., 1989, New K-Ar Age Dates, Geochemistry, and Stratigraphic Data for the Indian Heaven Quaternary Volcanic Field, South Cascade Range, Washington: Washington Division of Geology and Earth Resources Open-File Report 89-3, 42 p.
- Kuiper, K.F., Deino, A., Hilgen, F.J., Krijgsman, W., Renne, P.R., and Wijbrans, J.R., 2008, Synchronizing rock clocks of Earth history: Science, v. 320, p. 500–504, https://doi.org/10.1126/science.1154339.
- Laj, C., and Channell, J.E.T., 2007, Geomagnetic excursions, in Kono, M., ed., Treatise on Geophysics, Volume 5. Geomagnetism: Amsterdam, Netherlands, Elsevier, p. 373–416.
- Le Bas, M.J., Lemaitre, R.W., Streckeisen, A., and Zanettin, B., 1986, A chemical classification of volcanic-rocks based on the total alkali silica diagram: Journal of Petrology, v. 27, no. 3, p. 745–750, https://doi.org/10.1093/petrology/27.3.745.
- Leeman, W.P., Smith, D.R., Hildreth, W., Palacz, Z., and Rogers, N., 1990, Compositional diversity of late Cenozoic basalts in a transect across the southern Washington Cascades: Implications for subduction zone magmatism: Journal of Geophysical Research, v. 95, no. B12, p. 19,561–19,582, https://doi.org/10.1029/JB095iB12p19561.
- Leeman, W.P., Lewis, J.F., Evarts, R.C., Conrey, R.M., and Streck, M.J., 2005, Petrologic constraints on the thermal structure of the Cascades arc: Journal of Volcanology and Geothermal Research, v. 140, p. 67–105, https://doi.org/10.1016/j.jvolgeores.2004.07.016.
- Lisiecki, L.E., and Raymo, M.E., 2005, A Pliocene–Pleistocene stack of 57 globally distributed benthic  $\delta^{18}O$  records: Paleoceanography, v. 20, PA1003, https://doi.org/10.1029/2004PA001071.
- Longo, A.L., Dilles, J.H., Grunder, A.L., and Duncan, R., 2010, Evolution of calc-alkaline volcanism and associated hydrothermal gold deposits at Yanacocha, Peru: Economic Geology and the Bulletin of the Society of Economic Geologists, v. 105, no. 7, p. 1191–1241, https://doi .org/10.2113/econgeo.105.7.1191.
- Lund, S.P., Stoner, J.S., Channell, J.E.T., and Acton, G., 2006, A summary of Brunhes paleomagnetic field variability recorded in ODP cores: Physics of the Earth and Planetary Interiors, v. 156, p. 194–204, https://doi. org/10.1016/j.pepi.2005.10.009.
- Mahon, K.I., 1996, The new "York" regressions: Applications of an improved statistical method to geochemistry: International Geology Review, v. 38, p. 293–303, https://doi.org/10.1080/00206819709465336.
- Matthews, N.E., Vazquez, J.A., and Calvert, A.T., 2015, Age of the Lava Creek supereruption and magma chamber assembly at Yellowstone based on <sup>40</sup>Ar/<sup>39</sup>Ar and U-Pb dating of sanidine and zircon crystals: Geochemistry Geophysics Geosystems, v. 16, p. 2508–2528, https://doi.org/10.1002/2015GC005881.
- Michalk, D.M., Böhnel, H.N., Nowaczyk, N.R., Aguírre-Diaz, G.J., López-Martínez, M., Ownby, S., and Negendank, J.F.W., 2013, Evidence for geomagnetic excursions recorded in Brunhes and Matuyama chron lavas from the Trans-Mexican volcanic belt: Journal of Geophysical Research—Solid Earth, v. 118, p. 2648–2669, https://doi.org/10.1002/jgrb.50214.
- Michelfelder, G.S., Feeley, T.C., Wilder, A.D., and Klemetti, E.W., 2013, Modification of the continental crust by subduction zone magmatism and vice-

- versa: Across-strike geochemical variations of silicic lavas from individual eruptive centers in the Andean Central volcanic zone: Geosciences, v. 3, no. 4, p. 633–667, https://doi.org/10.3390/geosciences3040633.
- Miller, R.B., 1989, The Mesozoic Rimrock Lake inlier, southern Washington Cascades: Implications for the basement to the Columbia Embayment: Geological Society of America Bulletin, v. 101, p. 1289–1305, https://doi.org/10.1130/0016-7606(1989)101<1289:TMRLIS>2.3.CO;2.
- Min, K.W., Mundil, R., Renne, P.R., and Ludwig, K.R., 2000, A test for systematic errors in <sup>40</sup>Ar/<sup>39</sup>Ar geochronology through comparison with U/Pb analysis of a 1.1-Ga rhyolite: Geochimica et Cosmochimica Acta, v. 64, no. 1, p. 73–98, https://doi.org/10.1016/S0016-7037(99)00204-5.
- Mitchell, R.J., Jaeger, D.J., Diehl, J.F., and Hammond, P.E., 1989, Paleomagnetic results from the Indian Heaven volcanic field, south-central Washington: Geophysical Journal, v. 97, p. 381–390, https://doi.org/10.1111/j.1365-246X.1989.tb00509.x.
- Mullen, E.K., Weis, D., Marsh, N.B., and Martindale, M., 2017, Primitive arc magma diversity: New geochemical insights in the Cascade arc: Chemical Geology, v. 448, p. 43–70, https://doi.org/10.1016/j.chemgeo.2016.11.006.
- Mullineaux, D.R., and Crandell, D.R., 1981, The eruptive history of Mount St. Helens, *in* Lipman, P.W., and Mullineaux, D.R., eds., The 1980 Eruptions of Mount St. Helens, Washington: U.S. Geological Survey Professional Paper 1250, p. 3–15.
- Ownby, S., Granados, H.D., Lange, R.A., and Hall, C.M., 2007, Volcán Tancítaro, Michoacán, Mexico: <sup>40</sup>Ar/<sup>39</sup>Ar constraints on its history of sector collapse: Journal of Volcanology and Geothermal Research, v. 161, p. 1–14, https://doi.org/10.1016/j.jvolgeores.2006.10.009.
- Peter Hooper GeoAnalytical Laboratory, 2017, ICP-MS Method: Trace Element Analyses of Rocks and Minerals by ICP-MS: http://cahnrs.wsu.edu/soe/facilities/geolab/technotes/icp-ms\_method/ (accessed May 2017).
- Russell, I.C., 1893, A Geological Reconnaissance in Central Washington: Bulletin of the United States Geological Survey 108, 108 p.
- Savant, S., and de Silva, S.L., 2005, A GIS-based spatial analysis of volcanoes in the Central Andes: Insights into factors controlling volcano spacing: San Francisco, California, American Geophysical Union, 2005 Fall Meeting, abstract no. V21D–0648.
- Sawlan, M.G., 2018, Alteration, mass analysis, and magmatic compositions of the Sentinel Bluffs Member, Columbia River flood basalt province: Geosphere, v. 14, no. 1, p. 286–303, https://doi.org/10.1130/GES01188.1.
- Schaltegger, U., Schmitt, A.K., and Horstwood, M.S.A., 2015, U-Th-Pb zircon geochronology by ID-TIMS, SIMS, and laser ablation ICP-MS: Recipes, interpretations, and opportunities: Chemical Geology, v. 402, p. 89–110, https://doi.org/10.1016/j.chemgeo.2015.02.028.
- Schärer, U., 1984, The effect of initial <sup>230</sup>Th disequilibrium on young U-Pb ages: The Makalu case, Himalaya: Earth and Planetary Science Letters, v. 67, p. 191–204, https://doi.org/10.1016/0012-821X(84)90114-6.
- Schmidt, M.E., Grunder, A.L., and Rowe, M.C., 2008, Segmentation of the Cascade arc as indicated by Sr and Nd isotopic variation among diverse primitive basalts: Earth and Planetary Science Letters, v. 266, p. 166–181, https://doi.org/10.1016/j.epsl.2007.11.013.
- Scott, W.E., and Gardner, C.A., 2017, Field-Trip Guide to Mount Hood, Oregon, Highlighting Eruptive History and Hazards: U.S. Geological Survey Scientific Investigations Report 2017–5022-G, 115 p.
- Scott, W.E., Gardner, C.A., Sherrod, D.R., Tilling, R.I., Lanphere, M.A., and Conrey, R.M., 1997, Geologic History of Mount Hood Volcano, Oregon—A Field-Trip Guidebook: U.S. Geological Survey Open-File Report 97-263, 36 p.
- Shen, W., Ritzwoller, M.H., and Schulte-Pelkum, V., 2013, A 3-D model of the crust and uppermost mantle beneath the Central and Western US by joint inversion of receiver functions and surface wave dispersion: Journal of Geophysical Research–Solid Earth, v. 118, p. 262–276, https://doi. org/10.1029/2012JB009602.
- Sherrod, D.R., and Scott, W.E., 1995, Preliminary Geologic Map of the Mount Hood 30- by 60-Minute Quadrangle, Northern Cascade Range, Oregon: U.S. Geological Survey Open-File Report 95-219, 36 p., 1 plate.
- Singer, B.S., Hoffman, K.A., Chauvin, A., Coe, R.S., and Pringle, M.S., 1999, Dating transitionally magnetized lavas of the late Matuyama chron: Toward a new <sup>40</sup>Ar/<sup>39</sup>Ar timescale of reversals and events: Journal of Geophysical Research, v. 104, no. B1, p. 679–693, https://doi.org/ 10.1029/1998JB900016.
- Singer, B.S., Hoffman, K.A., Schnepp, E., and Guillou, H., 2008, Multiple Brunhes chron excursions recorded in the West Eifel (Germany)

- volcanics: Support for long-held mantle control over the non-axial dipole: Physics of the Earth and Planetary Interiors, v. 169, p. 28–40, https://doi.org/10.1016/j.pepi.2008.05.001.
- Sisson, T.W., Vallance, J.W., and Pringle, P.T., 2001, Progress made in understanding Mount Rainier's hazards: Eos (Washington, D.C.), v. 82, no. 9, p. 113, 118–120.
- Sisson, T.W., Salters, V.J.M., and Larson, P.B., 2014, Petrogenesis of Mount Rainier andesite: Magma flux and geologic controls on the contrasting differentiation styles at stratovolcanoes of the southern Washington Cascades: Geological Society of America Bulletin, v. 126, no. 1–2, p. 122– 144, https://doi.org/10.1130/B30852.1.
- Smith, D., and Leeman, W., 1987, Petrogenesis of Mount St. Helens dacitic magmas: Journal of Geophysical Research, v. 92, no. B10, p. 10,313– 10,334, https://doi.org/10.1029/JB092iB10p10313.
- Smith, G.O., 1903, Description of the Ellensburg Quadrangle, Washington: U.S. Geological Survey Atlas Folio 86, 7 p.
- Stacey, J., and Kramers, J.D., 1975, Approximation of terrestrial lead isotope evolution by a two-stage model: Earth and Planetary Science Letters, v. 26, p. 207–221, https://doi.org/10.1016/0012-821X(75)90088-6.
- Stanley, W.D., Finn, C., and Plesha, J.L., 1987, Tectonics and conductivity structures in the southern Washington Cascades: Journal of Geophysical Research, v. 92, no. B10, p. 10,179–10,193, https://doi.org/10.1029/JB092iB10p10179.
- Steenberg, L., Boroughs, S., and Knaack, C., 2017, Estimation of accuracy and precision for trace elements analyzed by inductively coupled plasma mass spectrometry (ICP-MS) at the Peter Hooper GeoAnalytical Laboratory, Washington State University: Geological Society of America Abstracts with Programs, v. 49, no. 6, paper no. 69-3, https://doi.org/10.1130/ abs/2017AM-307211.
- Swanson, D.A., 1966, Tieton volcano, a Miocene eruptive center in the Southern Cascade Mountains, Washington: Geological Society of America Bulletin, v. 77, p. 1293–1314, https://doi.org/10.1130/0016-7606 (1966)77[1293:TVAMEC]2.0.CO;2.
- Swanson, D.A., 1978, Geologic Map of the Tieton River Area, Yakima County, South-Central Washington: U.S. Geological Survey Miscellaneous Field Studies Map 968, scale 1:48,000.
- Swanson, D.A., 1996a, Geologic Map of the Hamilton Buttes Quadrangle, Southern Cascade Range, Washington: U.S. Geological Survey Open-File Report 96-0016, 29 p., 2 plates.
- Swanson, D.A., 1996b, Geologic Map of the Packwood Lake Quadrangle, Southern Cascade Range, Washington: U.S. Geological Survey Open-File Report 96-704, 25 p., 2 plates.
- Swanson, D.A., and Clayton, G.A., 1983, Generalized Geologic Map of the Goat Rocks Wilderness and Roadless Areas (6036, Parts A, C, and D), Lewis and Yakima Counties, Washington: U.S. Geological Survey Open-File Report 83-357, scale 1:48,000.
- Tamura, Y., Tatsumi, Y., Zhao, D., Kido, Y., and Shukuno, H., 2001, Distribution of Quaternary volcanoes in the Northeast Japan arc; geologic and geo-

- physical evidence of hot fingers in the mantle wedge: Proceedings of the Japan Academy, v. 77, p. 135–139, https://doi.org/10.2183/pjab.77.135.
- Taylor, J.R., 1997, An Introduction to Error Analysis: The Study of Uncertainties in Physical Measurements (2nd ed.): Sausalito, California, University Science Books, 327 p.
- ten Brink, U., 1991, Volcano spacing and plate rigidity: Geology, v. 19, no. 4, p. 397–400, https://doi.org/10.1130/0091-7613(1991)019<0397:VSAPR >2.3.CO;2.
- Trehu, A.M., Asudeh, I., Brocher, T.M., Luetgert, J.H., Mooney, W.D., Nabelek, J.L., and Nakamura, Y., 1994, Crustal architecture of the Cascadia forearc: Science, v. 266, p. 237–243, https://doi.org/10.1126/science.266.5183.237.
- Vazquez, J.A., and Lidzbarski, M.I., 2012, High-resolution tephrochronology of the Wilson Creek Formation (Mono Lake, California) and Laschamp event using <sup>238</sup>U-<sup>230</sup>Th SIMS dating of accessory mineral rims: Earth and Planetary Science Letters, v. 357–358, p. 54–67, https://doi.org/10.1016/j.epsl.2012.09.013.
- Walker, B.A., Klemetti, E.W., Grunder, A.L., Dilles, J.H., Tepley, F.J., and Giles, D., 2012, Crystal reaming during the assembly, maturation, and waning of an eleven-million-year crustal magma cycle: Thermobarometry of the Aucanquilcha volcanic cluster: Contributions to Mineralogy and Petrology, v. 165, no. 4, p. 663–682, https://doi.org/10.1007/s00410-012 -0829-2.
- Walker, G.P.L., 2000, Basaltic volcanoes and volcanic systems, in Sigurdsson, H., Houghton, B.F., McNutt, S.R., Rymer, H., and Stix, J., eds., Encyclopedia of Volcanoes: San Diego, California, Academic Press, p. 283–289.
- Wells, R.E., and McCaffrey, R., 2013, Steady rotation of the Cascade arc: Geology, v. 41, no. 9, p. 1027–1030, https://doi.org/10.1130/G34514.1.
- Wells, R.E., Weaver, C.S., and Blakely, R.J., 1998, Forearc migration in Cascadia and its neotectonic significance: Geology, v. 26, p. 759–762, https://doi.org/10.1130/0091-7613(1998)026<0759:FAMICA>2.3.CO;2.
- Wells, R.E., Bukry, D., Friedman, R., Pyle, D., Duncan, R., Haeussler, P., and Wooden, J., 2014, Geologic history of Siletzia, a large igneous province in the Oregon and Washington Coast Range: Correlation to the geomagnetic polarity time scale and implications for a long-lived Yellowstone hotspot: Geosphere, v. 10, no. 4, p. 692–719, https://doi.org/10.1130/GES01018.1.
- Wise, W.S., 1969, Geology and petrology of the Mt. Hood area: A study of High Cascade volcanism: Geological Society of America Bulletin, v. 80, p. 969–1006, https://doi.org/10.1130/0016-7606(1969)80[969:GAPOTM]2.0.CO;2.
- York, D., 1968, Least squares fitting of a straight line with correlated errors: Earth and Planetary Science Letters, v. 5, p. 320–324, https://doi.org/ 10.1016/S0012-821X(68)80059-7.

Manuscript Accepted by the Society 12 March 2018 Manuscript Published Online 10 July 2018